Benzoquinonediimine ligands: Synthesis, coordination chemistry and properties

Simon Pascal, Olivier Siri

Benzoquinonediimine ligands: synthesis, coordination chemistry and properties

Simon Pascal, Olivier Siri*

Aix Marseille Univ, CNRS, UMR 7325, CINaM, Campus de Luminy, case 913, 13288 Marseille cedex 09, France
E-mail: olivier.siri@univ-amu.fr

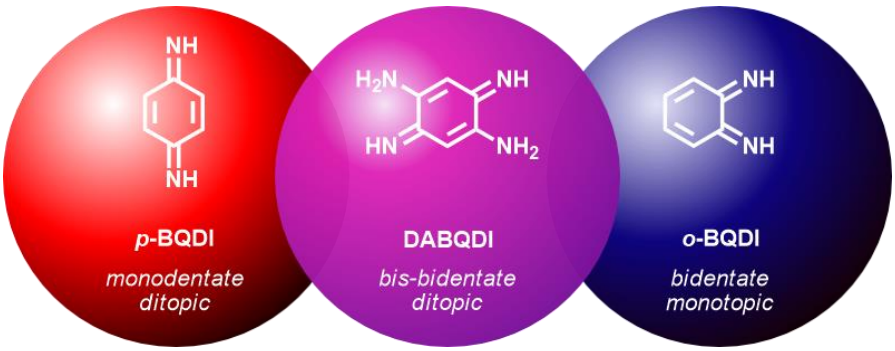

Abstract: This review covers the synthesis and properties of 2,5-diamino-1,4-benzoquinonediimines (DABQDI), and their use as ligand in coordination chemistry. Although reported more than a century ago, these molecules emerged as highly versatile ligands only from 1998, and are so far used for the synthesis of numerous complexes with remarkable properties. This exceptional versatility results from the possible tuning of the *N*-substituents and the observation of an isomerization process upon coordination depending on the metal center. As such, these DABQDI can be also considered as ligands that combine the structural elements of *ortho*- and *para*-benzoquinonediimines (*o*-BQDI and *p*-BQDI) which are bidentate monotopic and monodentate ditopic ligands, respectively. These two classes of BQDI ligands are also reviewed in order to parallel their properties to those of the complexes based on DABQDI.

1. Introduction and scope

Quinoidal molecules have received particular attention from chemists, physicists and biochemists as building block in the fields of dyes chemistry, conducting organic materials, supramolecular chemistry and pharmacology [1-6]. Over the last three decades, they have also been strongly investigated as ligand, for the design of complexes that could be used in a wide range of applications ranging from catalysis and molecular electronics, to magnetism or optics [7-10]. Among these quinoidal ligands, *para*- and *ortho*-benzoquinonediimines (*p*- and *o*-BQDI) have a long history because of their easy access and their different coordination mode (mono- *vs* bidentate) which allowed the preparation of numerous complexes (Chart 1). When 1,4-benzoquinonediimine (*p*-BQDI) is substituted in positions 2 and 5 by an amine function NH_2 (DABQDI), the coordination chemistry differs drastically and becomes much more versatile compared to *p*- and *o*-BQDI ligands because of the possible *p*→*o* isomerization of DABQDI. As a consequence, this latter can be considered as a ligand that combines the structural elements of these two BQDI which are bidentate monotopic and monodentade ditopic ligands, respectively. Curiously, DABQDI can be considered as an emerging class of versatile ligands by comparison with its oxygenated analogue (2,5-dihydroxy-1,4-benzoquinone DHBQ, see Chart 1) which has been extensively used in coordination chemistry for decades. The possible presence of *N*-substituents enlarges indeed the scope of these N_4 ligands for embracing new challenging areas. The present review is the first attempt that aims to summarize the coordination chemistry of these three types of benzoquinonediimine ligands.

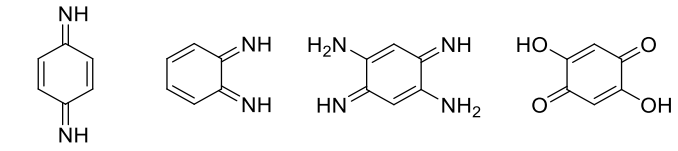

***p*-BQDI**	***o*-BQDI**	**DABQDI**	**DHBQ**
monodentate ditopic	*bidentate monotopic*	*bis-bidentate ditopic*	*bis-bidentate ditopic*

Chart 1. Benzoquinonediimines under the scope of this review and structure of dihydroxybenzoquinone.

In a first part, special attention will be devoted to the richness of the coordination chemistry of *para*- and *ortho*-benzoquinonediimines (*p*- and *o*-BQDI). While the position of the nitrogen atom within ditopic *p*-BQDI is ideal to develop conjugated complexes, the interest of *o*-BQDI isomer mainly lies in its bidentate character and multiple redox states. The second part will focus on the use of DABQDI (with or without *N*-substituents) as a versatile ditopic and bis-bidentate *N*-ligand for the design of coordination complexes featuring unique physico-chemical properties. These latter are relevant in several technological sectors, *e.g.* catalysis [11-13] or molecular materials (wires, switches, memories, …) [14], by analogy with the well-known non-innocent ligands and mixed-valence complexes. The coordination and electronic assets let foresee a tremendous potential since this type of ligands can be employed to develop polynuclear and conjugated complexes. Particular emphasis will be given to the optical and redox properties of the metal ligand complexes. Aside, the synthetic pathways to access these ligands

and modify their substitution will be also described in order to highlight the versatility of this fascinating class of 12π-electrons quinones.

2. *Coordination chemistry of para*- and *ortho*-benzoquinonediimines

Para- and *ortho*-benzoquinonediimines (Chart 1) are respectively obtained from *p*- and *o*-phenylenediamine (PDA) following chemical, aerobic or metal-assisted oxidation of the species. Historically, these precursors are already well-known as oxidative hair colorants (for more than a century) [15, 16] or as precursors for the synthesis of numerous dyes such as phenazines and azaacenes [17-22], which found several applications, notably as chemical and biological probes or in organic electronics [23-25]. Although the metalation of BQDI has been already reviewed, this section aims to exemplify their use as ligand in coordination chemistry and the diversity of the obtained complexes which will figure as basis for further description of DABQDI-based architectures (see Section 4).

2.1. *p*-benzoquinonediimine ligands

Ludi and co-workers reported in 1975 the coordination of ruthenium(II)pentaamine with *p*-BQDI (Scheme 1) [26]. A tricationic complex **1•H$^+$** was isolated as purple crystals, featuring intense visible absorption centered at 522 nm. The dramatic red-shift of absorption compared to the free diimine ligand (λ_{max} = 322 nm) is attributed to a ligand-to-metal charge transfer (LMCT) process. Disappearance of this transition is monitored upon two-electron reduction of complex **1•H$^+$**, which presumably generates the aromatic form of the ligand (λ_{max} = 286 nm). Deprotonation of complex **1•H$^+$** occurred in basic aqueous solution, generating the dicationic species **1**, featuring red-shifted absorption maximum at 562 nm, presumably due to increased LMCT. A p*K*a of 10.6 was determined for this system, which underlines the higher basicity of the complex compared to the free *p*-BQDI ligand (p*K*a = 5.75). Furthermore, the introduction of methyl groups at the iminium extremity (**2a**) and extension of conjugation using a central naphthalene ring (**3**) are efficient methods to further red-shift the absorption up to the orange spectral range (λ_{max} = 568 and 599 nm, respectively). Afterwards, the same group reported in 1985 analogous complexes introducing osmium(II) (**2b**), and consequently evidenced the negligible effect of the transition metal on the absorption properties [27].

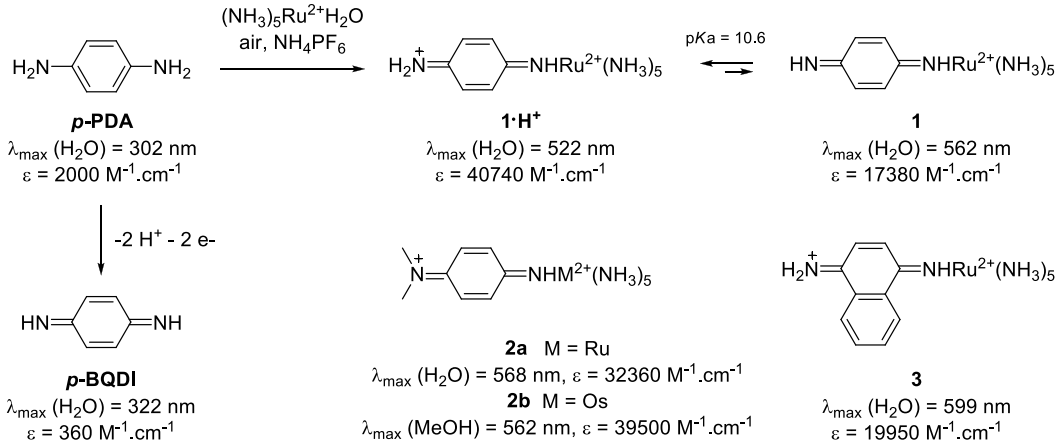

Scheme 1. Complexes of *p*-BQDI and corresponding lower energy absorption characteristics [26, 27].

In 1981, Ludi *et al.* managed to prepare a dinuclear ruthenium complex incorporating a *p*-BQDI bridge (**4**, Figure 1) by mixing *p*-PDA in an aqueous solution of $[(NH_3)_5Ru(H_2O)]^{2+}$ [28]. Interestingly, the absorption spectrum of **4** exhibits three intense low energy bands in the red and near-infrared (NIR) ranges which were attributed to intervalence charge transfer (IVCT) transitions [29]. Cyclic voltammetry of **4** in acetonitrile/water reveals oxidation and reduction at 0.82 and 0.21 V *vs*. NHE, respectively, while the reduction of the *p*-BQDI ligand to *p*-PDA presumably occurs *ca*. -1 V. The comproportionation equilibrium was estimated to be shifted towards formation of the mixed-valence complex (K_{com} ~ 10^{10}). Moreover, combined NMR, EPR and crystallographic analysis corroborated the mixed-valence nature of this *p*-BQDI-bridged Ru(II)/Ru(III) complex.

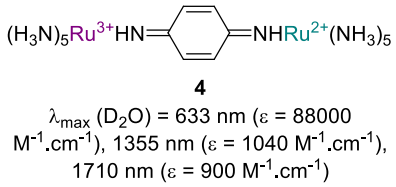

Figure 1. Structure of dinuclear complex **4** [28].

Herington reported in 1959 the synthesis of linear $[(CN)_5Fe•HN\text{-}C_6H_4\text{-}NH•Fe(CN)_5][Zn_3]$ from *p*-phenylenediamine and a disodium pentacyanoamminoferrate precursor in aqueous NaOH solution. However the poor solubility of the complex did not permit the investigation of its properties in solution [30]. In 1991, a novel synthetic procedure allowed to isolate this dinuclear complex as a water-soluble sodium salt **5a** (Scheme 2) [31]. Upon lowering the pH, conversion to the mononuclear complex **6** was evidenced, accompanied by a slight hypsochromic shift of the absorption maximum to 676 nm. Further acidification of the solution triggered the protonation of the BQDI ligand and a red-shift of the absorption towards the far red region (λ_{max} = 725 nm for **6•H$^+$**). Unlike the system **1**, which LMCT transition undergoes blue-shift upon protonation, the lower energy transition in **6** is attributed to a metal-to-ligand charge transfer (MLCT), transition which is therefore shifted to lower energy upon protonation.

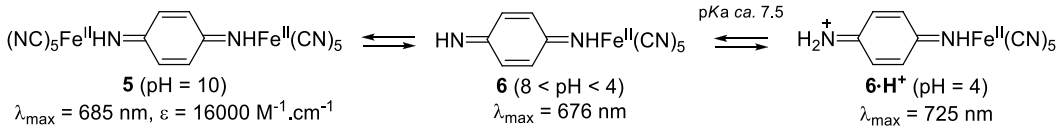

Scheme 2. Dinuclear and mononuclear complexes of *p*-BQDI pentacyanoferrate [31].

Hirao, Moriuichi and co-workers developed numerous π-conjugated complexes introducing *N*-substituted *p*-BQDI **7** (*N*,*N*-bis(4'-aminophenyl)-1,4-quinonediimine) [32] ligands as bridging spacers (Scheme 3) [33]. On the one hand, using a Pd precursor bearing a tridentate ligand (**11a**), a bimetallic complex **8a** was obtained [34]. This conjugated complex that exhibits absorption centered in the NIR region (λ_{max} = 806 nm) could be reversibly and stepwise reduced: first to the corresponding semiquinone diamine **8a**$^{\bullet-}$ (λ_{max} = 931 nm), and secondly to the phenylenediamide dianion **8a**$^{2-}$ (no absorption details). EPR analysis of **8a**$^{\bullet-}$ shows that the *p*-BQDI bridge behaves as a non-innocent ligand since the unpaired electron is mainly localized on the ligand and weakly delocalized on the Pd nucleus (Figure 2). On the other hand, while the reaction of ligand **7** with $[PdCl_2(MeCN)_2]$ induces the polymerization of the complex (**9**), treatment with an ethylenediamine-Pd(II) precursor leads to the formation of the trimetallic macrocyle **10**, featuring a broad absorption transition centered *ca.* 800 nm [35].

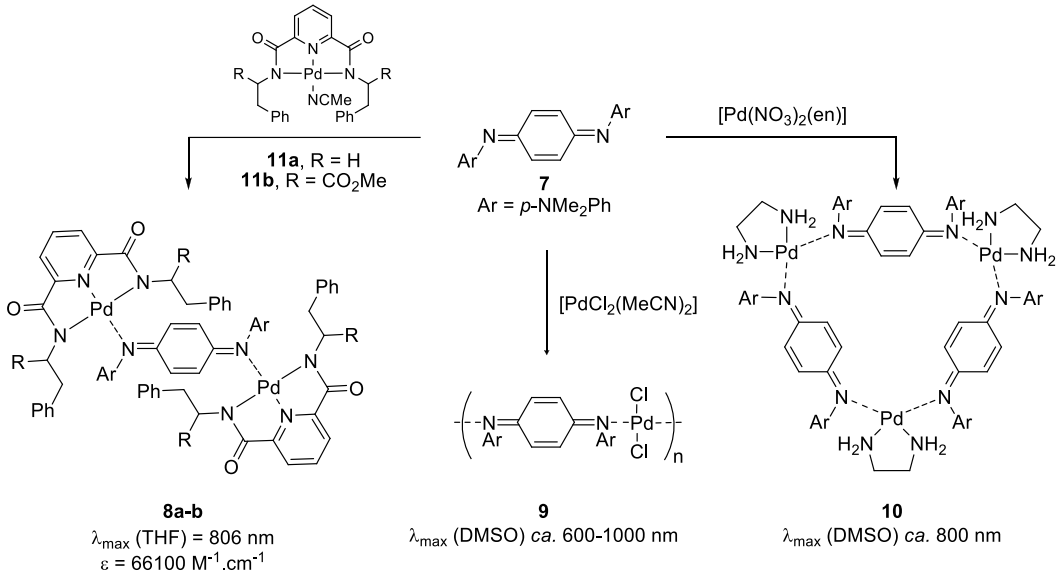

Scheme 3. Conjugated polynuclear Pd complexes introducing *p*-BQDI ligands [34, 35].

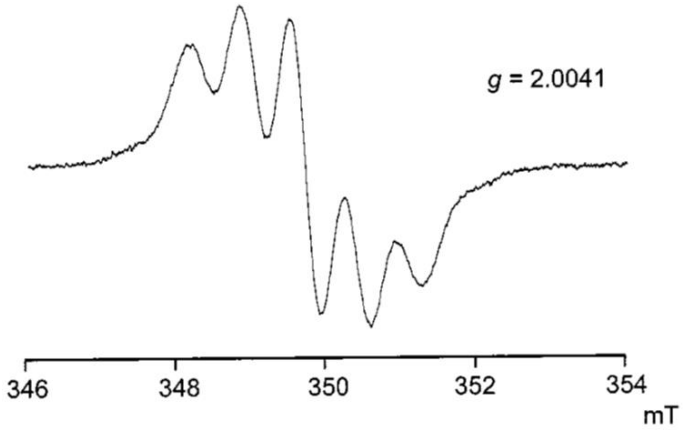

Figure 2. EPR spectrum of **8a**$^{\bullet-}$ in THF at 290K. Reproduced with permission from Ref. [34].Copyright WILEY-VCH Verlag GmbH, 2001.

Coordination complexes analogue to **8** found a particular interest in the development of chiral conducting polymers [36]. Similar architectures were developed using the chiral tridendate ligand **11b** to obtain conjugated dinuclear complex **8b** exhibiting electronic circular dichroism (ECD), induced by the complexation to the quinoidal ligand, up to the NIR spectral region (Figure 3) [37, 38].

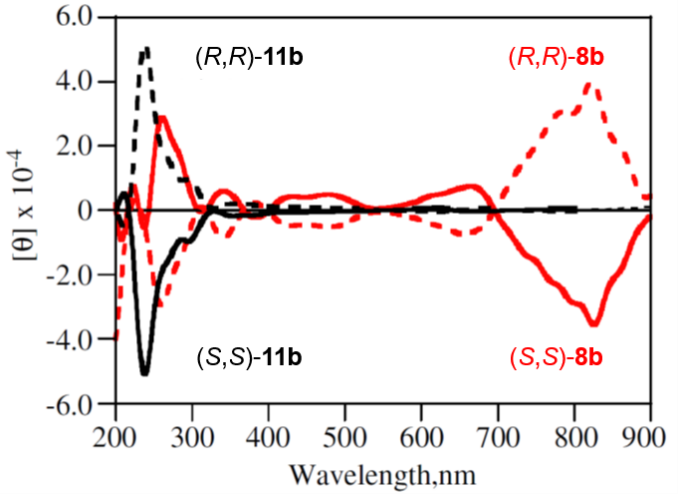

Figure 3. UV-Vis-NIR ECD spectra of ligand **11b** (10^{-4} M) and complex **8b** (5.10^{-5} M) in CH_2Cl_2. Figure was reproduced from ref. [37] with permission of the copyright holders.

Finally, beyond the scope of the simple *p*-BQDI ligand, it is worthy to note that the same collaborators reported vanadium(IV) complexes of emeraldine [39] and investigated the redox switching of various polyaniline and quinonediimine derivatives introducing ruthenium bipyridine [40-42] or ferrocene extremities [43, 44].

2.2. *o*-benzoquinonediimines ligands

While only few works relate the use of *p*-BQDI as ligand, the *o*-BQDI isomer has been reported in a wider range of studies and its coordination chemistry has been extensively reviewed previously [11, 14,

45-48]. The attraction for such quinone is mainly explained by the fact that *o*-BQDI is a well-established non-innocent ligand (Scheme 4), *i.e.* it exhibits multiple redox states that enrich possible electron transfer within metal complexes. As such, these redox-active ligands can act as electron reservoirs to tune the electronic properties of a metal catalyst and/or play a role in catalytic processes [11-13]. Moreover, several ruthenium-based complexes featuring *o*-quinone ligands have found potential interest in biology as DNA-binding or cytotoxic agents [49-51]. In consequence, only few instances will be presented, with principal aim to establish a comparison basis with complexes introducing DABQDI ligands (see Section 4).

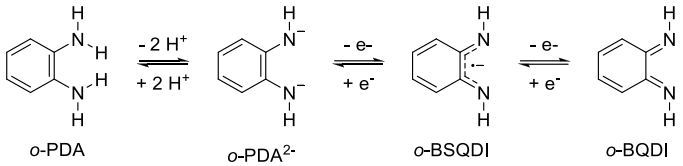

Scheme 4. Redox forms associated with *o*-phenylene diamine (*o*-PDA): dianion (*o*-PDA^{2-}), *o*-benzosemiquinone diimine (*o*-DBSQ) and *o*-benzoquinonediimine (*o*-BQDI).

Seminal work from Feigl and Fürth in 1927 reports the formation of a violet complex upon mixing Ni^{2+} and *o*-phenylenediamine (*o*-PDA) in aqueous ammonia [52]. Further mass spectrometry investigations of the complex and of those of other metal centers (Pd, Pt, Co analogues **13-15**) evidenced the structure of neutral $Ni[C_6H_4(NH)_2]_2$ **12** [53-55]. Even if the first proposition of the chemical structure of these complexes was described as its aromatic form, questions have been raised in 1955 concerning the possibility of a quinonediimine form of the ligand, according to Bardodej [56]. This hypothesis could be confirmed based on a crystallographic analysis of **12** that demonstrated a quinoidal character of the ligands in view of the bond length alternation within the $C_6H_4(NH)_2$ cycles (see **16** in Chart 2) [57]. Polarography experiments of diamagnetic series **12-15** revealed reversible one-electron oxidations and reductions leading respectively to the $[M\text{-}N_4]^{2+}$ and $[M\text{-}N_4]^{2-}$ species. These results paved the way in 1975 for the use of these complexes in semiconducting metal-organic salts [58]. Absorption measurements in DMSO solution highlight the particularly low energy bands located in the NIR range for Ni, Pd and Pt complexes, and up to 1135 nm for the Co derivative. In the case of nickel complex **12**, it was shown that substitution of one nitrogen of the ligand with a phenyl ring lead to exceptional batchochromic and hyperchromic shifts of the absorption, with a maximum at 823 nm for **17** [59]. In this instance, the authors presumed that complex **17** introduces two *o*-BSQDI ligands that could be successively and reversibly reduced to the generate Ni(*o*-BSQDI)(*o*-$PDA)^-$ then Ni $(o\text{-}PDA)_2^{2-}$ species at -0.69 and -1.37 V *vs.* Ag/AgCl, respectively.

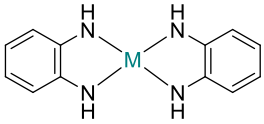

12, M = Ni
λ_{max} = 790 nm, ε = 54900 $M^{-1}.cm^{-1}$
13, M = Pd
λ_{max} = 780 nm, ε = 48200 $M^{-1}.cm^{-1}$
14, M = Pt
λ_{max} = 782 nm, ε = 3310 $M^{-1}.cm^{-1}$
15, M = Co
λ_{max} = 1135 nm, ε = 3840 $M^{-1}.cm^{-1}$

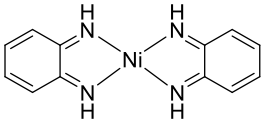

16

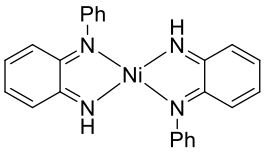

17
λ_{max} (MeCN) = 823 nm
ε = 416900 $M^{-1}.cm^{-1}$

Chart 2. Series of [M-N_4] type complexes **12-15** reported by Balch and Holm (absorption in DMSO) [55], structures of Ni[$C_6H_4(NH)_2]_2$ **16** [57] and *N*-substituted analogue **17** [59].

In 1973, Goedken and Christoph reported the isolation of a purple (*o*-BQDI)tetracyanoiron(II) complex and established the quinoidal nature of the ligand for this type of complex [60]. Shortly afterwards, Warren published a comparative study of *o*-BQDI complexes, including cobalt (**18**) and iron (**19**) derivatives (Chart 3), the former being obtained either from tris complex **20** or by oxidation of **15** in presence of sodium iodide [61]. Such series allows to highlight that the first oxidation potentials of complexes **16**, **18** and **19** was highly dependent on the metal, in the following order: Ni (+0.11 V) < Co (-0.15 V) < Fe (-0.36 V) in acetonitrile, their first reduction potential being located in a smaller range (-0.78 to -0.89 V *vs.* SCE). The series of hexacoordinated complexes **20-22** were described as colorful compounds and display strong absorption in the red region, the lower energy transition being attributed to a MLCT [62]. By comparison with bipyridine (bipy) ligand, *o*-BQDI is easier to reduce and therefore acts as a stronger π-acceptor. The particularly efficient π-backbonding has been studied in depth by Lever *et al.* in the case of $Ru^{II}[(NH_3)_2Cl_2$(*o*-BQDI)] complex [63, 64]. Interestingly, this complex was also reported to undergo disproportionation in presence of acid to yield $Ru^{III}[(NH_3)_2Cl_2$(*o*-BQDI)]$^+$ and $Ru^{III}[(NH_3)_2Cl_2$(*o*-PDA)]$^+$ [65]. Such proton-induced and pH-dependent disproportionation may find potential interest in the screening of catalytic and biological processes involving non-innocent ligands. Mixed complexes introducing *o*-PDA and *o*-BQDI ligand were successively reported: increasing the number of aromatic ligand in $Ru[(BQDI)_x$(*o*-$PDA)_{3-x}][PF_6]_2$ being principally accompanied by a blue-shift of the absorption (λ_{max} = 544 and 468 nm for x = 2 and 1, respectively) [66, 67].

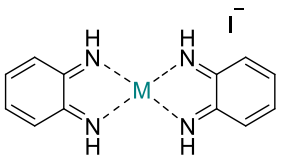

18, M = Co
λ_{max} = 751 nm, ε = 7600 $M^{-1}.cm^{-1}$
19, M = Fe
λ_{max} = 593 nm, ε = 14600 $M^{-1}.cm^{-1}$

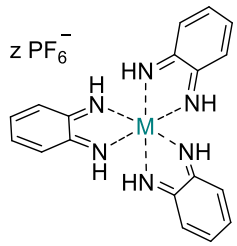

20, M = Co, z = 1
λ_{max} = 769 nm, ε = 10000 $M^{-1}.cm^{-1}$
21, M = Fe, z = 2
λ_{max} = 701 nm, ε = 17200 $M^{-1}.cm^{-1}$
22, M = Ru, z = 2
λ_{max} = 671 nm, ε = 12700 $M^{-1}.cm^{-1}$

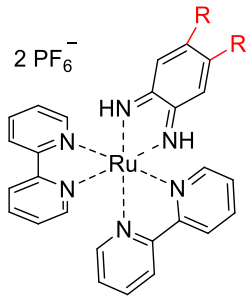

23, R = OCH_3
λ_{max} = 667 nm, ε = 251 $M^{-1}.cm^{-1}$
24, R = CH_3
λ_{max} = 730 nm, ε = 214 $M^{-1}.cm^{-1}$
25, R = H
λ_{max} = 752 nm, ε = 550 $M^{-1}.cm^{-1}$
26, R = Cl
λ_{max} = 791 nm, ε = 117 $M^{-1}.cm^{-1}$

Chart 3. Bis and tris *o*-BQDI complexes and absorption data in MeCN [61, 68].

Substitution of the quinonediimine ligand within structures **23-26** depicted in Chart 3 is accompanied by absorption and redox potential shifts that can be correlated to the corresponding Hammett parameters for each substituent [64, 68]. Not surprisingly, easier reductions are measured with increasing electron-withdrawing functions, together with bathochromic shift of the lower energy transition, characterized by a quite low extinction coefficients (ε < 600 $M^{-1}.cm^{-1}$). Controlled reduction allowed to record the absorption spectra of the *o*-BSQDI and *o*-PDA forms of the ligand, revealing non-negligible optical shifts. The authors were able to ascribe most of the transitions observed, the lower energy band in **25** (R = H, band 5 in Figure 4) being for instance attributed to a MLCT, and the second transition (*ca.* 500 nm, band 4 in Figure 4) having a mixed distribution between ligand and metal (defined as a metal-ligand to metal-ligand transition (MLML)). While, the reduction to the *o*-BSQDI ligand triggers the apparition of absorption transitions at 900 and 625 nm (bands 10 and 9, Figure 4), further reduction to the *o*-PDA form of the ligand leads to a blue-shift of the absorption maximum to 478 nm (band 13, Figure 4). The reader interested in the rationalization and tuning of the *o*-BSQDI ligand is invited to consult works by Wieghardt *et al.* that deliver complete experimental and theoretical investigations of semiquinone-based iron, ruthenium, cobalt, nickel and palladium complexes [69-74].

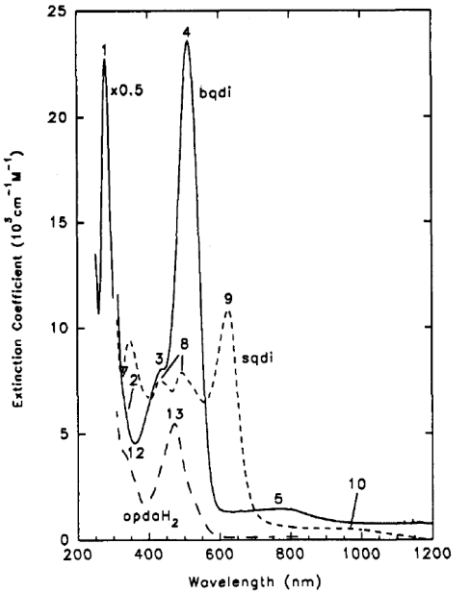

Figure 4. Absorption spectra of complexes $[Ru(bipy)_2(o\text{-PDA})]^{2+}$ (dashed line), $[Ru(bipy)_2(o\text{-BSQDI})]^{+}$ (dotted line) $[Ru(bipy)_2(o\text{-BQDI})]^{2+}$ (plain line) in MeCN. Reprinted with permission from Ref. [68]. Copyright1993 American Chemical Society.

3. Synthesis and properties of 2,5-diamino-benzoquinonediimines

3.1. Synthesis

3.1.1. Oxidation of tetraaminobenzene

By comparison with *o*- and *p*-PDA, tetraaminobenzene (TAB) is a highly electron rich aromatic compound that is potentially of great interest for the development of organic architectures and coordination complexes. However, the prompt aerial oxidation to DABQDI does not facilitate its usage but reveals instead to be a convenient method to access quinoidal systems. Historically, Nietzki brought to light the spontaneous oxidation of TAB under aerobic conditions in 1887 [75, 76]. Nakata *et al.* reported in 2005 the sublimation of unsubstituted DABQDI on a CsI plate cooled by closed-cycle refrigeration at 15 K but the compound was not fully characterized [77]. Although this molecule was first mentioned 130 years ago, the synthesis and full characterization of the unsubstituted DABQDI ligand has been published only in 2014 (Scheme 5) [78], the key feature being the precipitation of DABQDI in MeOH right after its formation in order to prevent further side reactions (hydrolysis, reaction with TAB, further oxidation…).

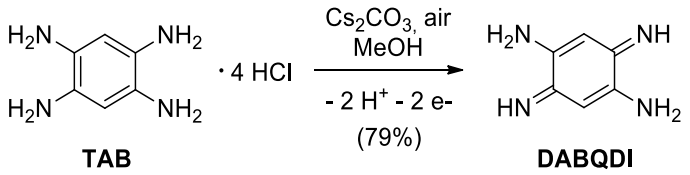

Scheme 5. Aerobic synthesis of DABQDI from TAB [78].

3.1.2. Self-condensation of anilines

Structures derived from DABQDI have been source of many discussions since the end of the nineteenth century, especially during the development of the indulines and other parent dyes derived from anilines [79]. Historically, the first example of DABQDI derivative was the azophenine **27** depicted in Scheme 6, which formation occurs through self-condensation of aniline with poor yield due to the production of several by-products. If this quinone was discovered by Kimich in 1875, its constitution formula was only established in 1888 by Fischer and Hepp [80, 81]. The next year, Bandrowski's work on the oxidation of *p*-PDA led to the isolation of the famous base named after him (Scheme 6) [82]. The structure of Bandrowski's base **28** was proposed by Green in 1913 and elucidated by Lauer 25 years later [83-85]. Aspects of this compound were intensively studied during the twentieth century due to occurrences in hair dyeing related dermatitis [86-88]. More recently, crystal structures of **27** and **28** have been reported, bringing an ultimate characterization of these historical DABQDI derivatives (Figure 5) [89, 90]. Interestingly, two molecular structures of azophenine **27** were reported as triclinic and orthorhombic polymorphs, showing different orientation of the phenyl rings and stabilized by weak C-H···π interactions or π-π stacking in the crystal, respectively [89, 91].

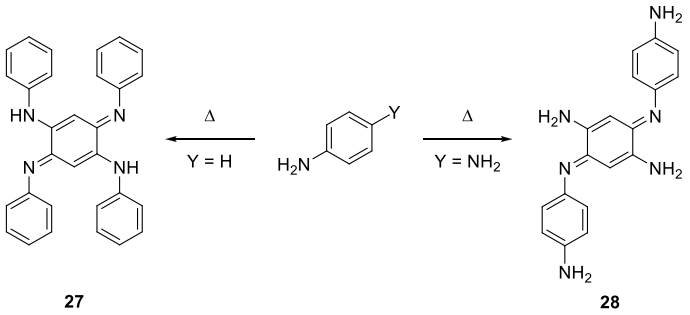

Scheme 6. Synthesis of historical DABQDI derivatives [80, 82].

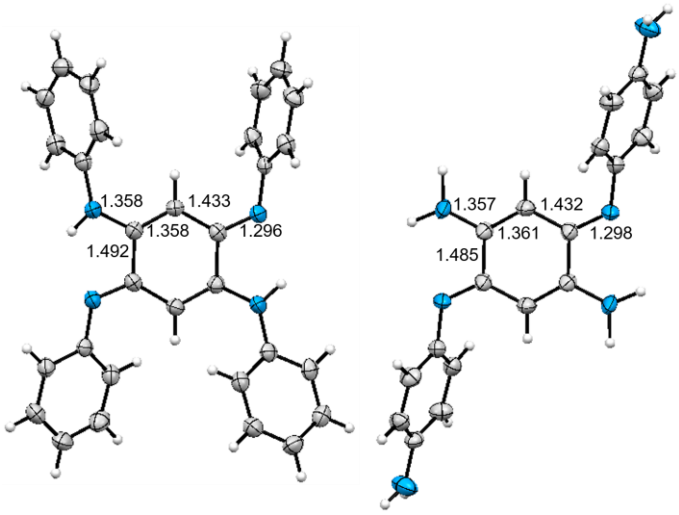

Figure 5. Structure and selected bond lengths (Å) of azophenine **27** (left, [89]) and Bandrowski's base **28** (right, [90]); Anisotropic displacement parameters at 50%.

3.1.3. Acylation reaction

Several general strategies were reported for the introduction of substituted amines on DABQDI. Although the DABQDI, azophenine and Bandrowski's base have been known for more than a century, the first alternative to prepare *N*-substituted analogues has been only reported in 2000 by Braunstein and Siri [92, 93]. This method - depicted in Scheme 7 - lies in the substitution of TAB using an acyl chloride reagent to form the aromatic derivative **29-a-c**. The resulting amide functions are reduced in presence of $LiAlH_4$, providing the intermediate **30a-c** which undergoes spontaneous oxidation during aerobic workup, by analogy with TAB. Functionalized quinones **31a-c** are then isolated with moderate to good yields mainly depending on the steric influence of the amide substituents.

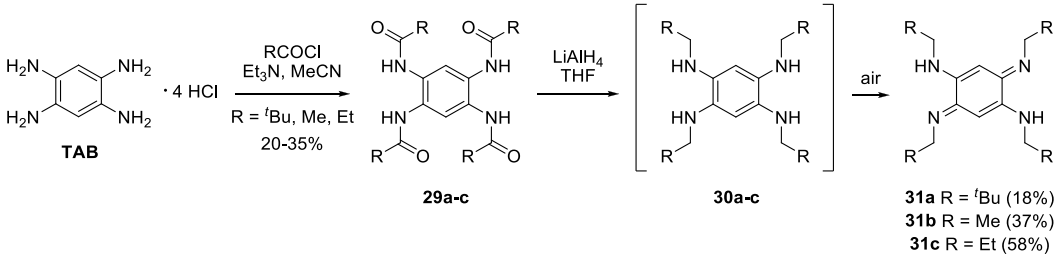

Scheme 7. Acylation of TAB to access *N*-substituted DABQDI derivatives [92, 93].

Aside, a multi-step procedure from diamino-dinitro-benzene derivatives allowed to access unsymmetrically *N*-substituted DABQDI (Scheme 8) [94]. Acylation of 4,5-dinitrobenzene-1,2-diamine (**32**) leads to the formation of compound **33** with an excellent yield, this latter being converted to **34** using $SnCl_2$ as reducing agent. Treatment with a different acyl chloride allows to form tetraamidobenzene **35** which does not undergo aerobic oxidation because of the electron-withdrawing amide functions. Their reduction with $LiAlH_4$ converts **35** into its corresponding tetraamine **36** (not isolated), that is readily oxidized in presence of air to yield the target quinone **37** as a yellow solid.

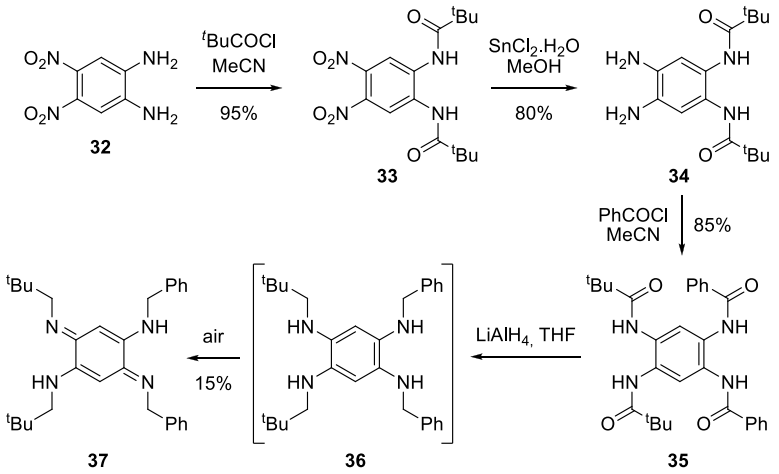

Scheme 8. Access to unsymmetrical *N*-substituted DABQDI derivatives [94].

3.1.4. Buchwald-Hartwig coupling reaction

An alternative method of *N*-functionalization is based on the direct coupling of amines on the tetrabromobenzene precursor **38** using the Buchwald-Hartwig reaction [95-97]. *N*-alkyl and *N*-aryl derivatives **39** are obtained with good to quasi-quantitative yields (Scheme 9). Interestingly, the nature of the substitution appears to influence the rate of aerobic oxidation to the corresponding quinone **40**: while the conversion occurs within few hours for arylamine derivatives, few days are necessary for the oxidation of the alkylamine analogues. By analogy with TAB tetrachloride, the oxidation of arenes **39** to quinones **40** can be prevented through protonation of the nitrogen atoms with HCl before their isolation.

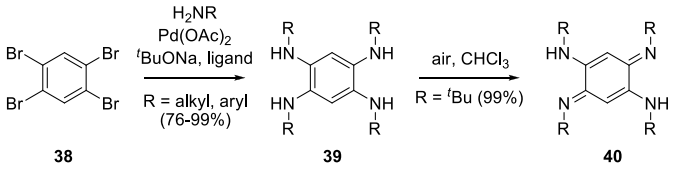

Scheme 9. *N*-substituted DABQDI *via* Pd(II) cross-coupling reaction [96].

3.1.5. Michael addition

Harvey and co-workers have recently disclosed a new pathway towards *N*-substituted DABQDI [98]. The *p*-benzoquinone reacted with the aniline derivative **41** in presence of excess $TiCl_4$ and a base to yield quinone **42** (Scheme 10). The synthon **42** was relevant to study the excited state of an emeraldine model and has later been used for the preparation of luminescent azophenine-Pt organometallic complexes [99].

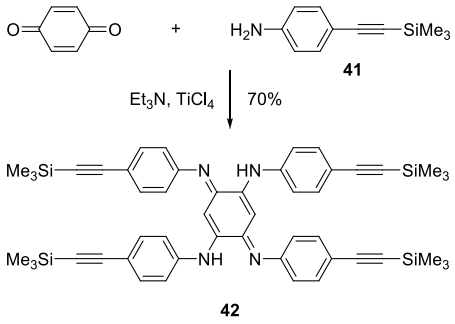

Scheme 10. Preparation of DABQDI from *p*-benzoquinone [98].

3.1.6. Transamination reaction

A particularly efficient and simple synthesis of *N*-substituted DABQDI based on transamination was recently reported (Scheme 11) [100]. During the reaction pathway, TAB tetrachloride is deprotonated in presence of a primary alkylamine and oxidized under air to the corresponding quinone. The

ammonium formed during the first step is crucial for the further generation of a charged iminium intermediate which yields product **40** *via* transamination. This atom-efficient method allowed to introduce various alkylamines without using any metal catalyst.

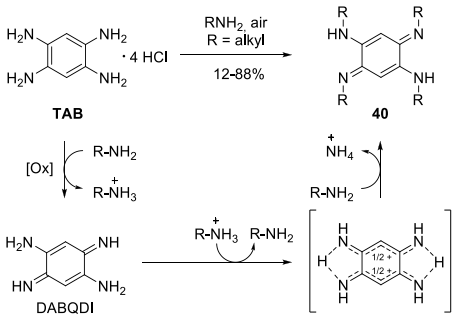

Scheme 11. *N*-substituted DABQDI *via* transamination [100].

3.1.7. Methylation and aminomethylenation of TAB

Eventually, the formation of charged DABQDI is conceivable by direct methylation or aminomethylenation of the TAB precursor. Staab and co-worked performed an Eschweiler-Clarke reaction in order to reach tetrakis(dimethylamino)benzene **43** incorporating four tertiary amines (Scheme 12) [101]. Following chemical or aerobic oxidation, the bis-cationic quinone **44** was isolated as a black-violet crystals (λ_{max} = 573 nm in acetonitrile). Analogous derivatives have more recently been obtained from the reaction of perfluorobenzene with various lithium dimethylamides to form **45**, followed by protodefluorination to reach **43** [102].

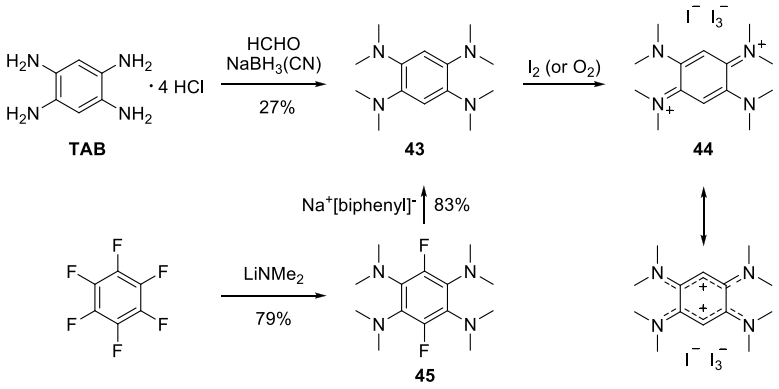

Scheme 12. Access to octamethyl-TAB and the corresponding diamino-benzoquinonediiminium salt [101, 102].

In a different way, Himmel *et al.* reported an original strategy to access tetrakis(tetramethylguanidino)benzene **46** by treatment of TAB with *N*,*N*,*N*′,*N*′-tetramethylformamidinium chloride (Scheme 13) [103]. This relatively stable molecule was then oxidized by iodine to yield the corresponding purple charged quinone **47** (λ_{max} *ca.* 350-470 nm in acetonitrile).

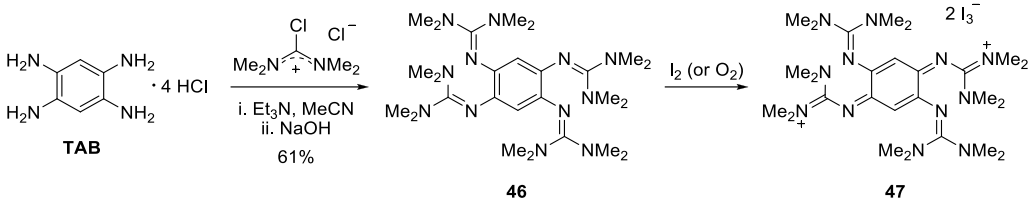

Scheme 13. Aminomethylenation of the TAB [103].

3.1.8. Synthesis from benzothiadiazole

Direct *C*-functionalization of DABQDI is so far unknown, however it is possible to access indirectly to these derivatives *via* a TAB precursor. Even if possibilities to access *C*-functionalized TAB remain scarce, few examples demonstrate a versatile approach based on the benzothiadiazole platform **48** [104-108]. This precursor is converted to the 4,7-dibromo-5,6-dinitrobenzothiadiazole **49** which can be coupled with a thiophene unit to from **50** (Scheme 14). The thiadiazole heterocycle and the nitro functions are finally reduced in the same step in presence of Zn and acetic acid. Because of its inherent unstability, compound **51** was directly condensed to diketone derivatives to access various quinoxaline dyes. However, we can reasonably expect its oxidation into *C*-substituted DABQDI **52** according to all the previous works on the oxidation of tetraaminobenzene derivatives.

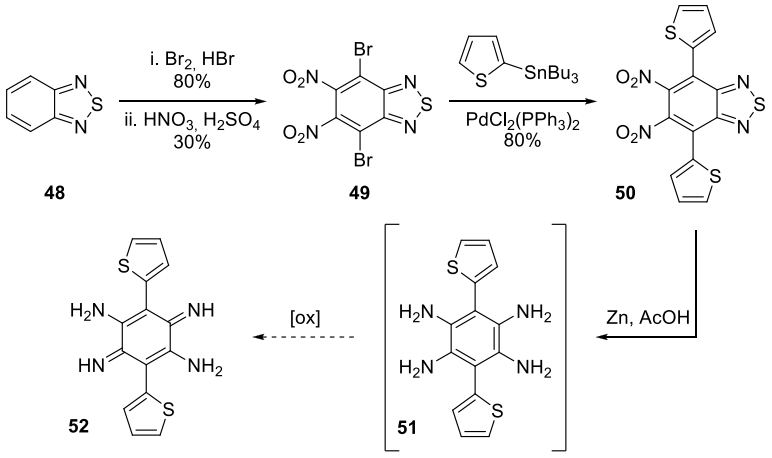

Scheme 14. Benzothiadiazole-based strategy to access *C*-functionalized TAB [104].

This hypothesis is consolidated by a recent work published in 2015 by Bunz *et al.* who reported a synthesis of ethynyl-functionalized DABQDI **56** based on two successive reductions of bis-benzothiadiazole **53** using $LiAlH_4$ to yield **54**. A mixture of $LiAlH_4$/Cu (4:1) finally allows to reach quinone **56**, whose formation results probably from the aerobic oxidation of its tetraamine aromatic precursor **55** (not isolated) (Scheme 15) [109]. Such functionalized platform has been used for the convenient generation of various azaacenes by condensation with *o*-quinones.

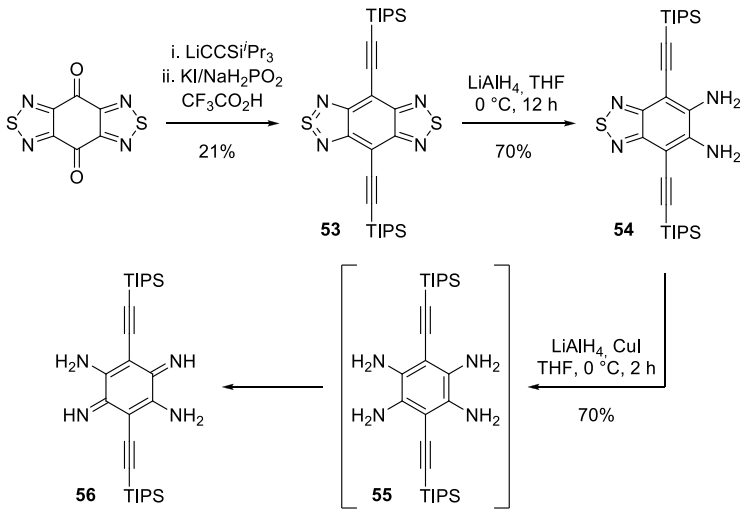

Scheme 15. Strategy to access ethynyl-functionalized DABQDI [109, 110].

It is noteworthy that strategies based on benzothiadiazole precursors to access a variety of *C*-functionalized DABQDI let foresee tremendous possibilities, especially in view of the numerous efficient methods reported for the functionalization of benzothiadiazoles [111, 112].

3.2. Properties of DABQDI

3.2.1. Tautomerism

It is well-established that the azophenine quinone and related DABQDI are subject to a double-proton transfer involving two possible tautomers, as presented in Scheme 16. This fast exchange has been characterized in solution and at the solid state using ^{1}H and ^{15}N NMR experiments [113]. Moreover, IR spectroscopy and theoretical calculations demonstrated that this isomerization could be triggered by UV-light irradiation [77].

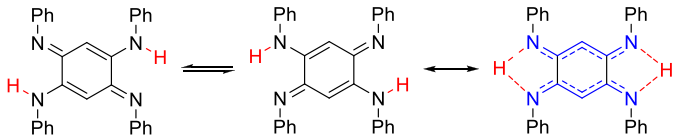

Scheme 16. Tautomeric equilibria of azophenine **27** in solution.

3.2.2. Acidochromism

In 1966, Dähne and Leupold predicted the so-called “coupling principle” in organic dyes to rationalize the unique spectroscopic properties of molecules incorporating 12π-electrons, that are best described as constituted of two 6π-subsystems chemically linked by two C-C single bonds but electronically independent [114]. Quinone **31a** (Scheme 17) perfectly illustrates this principle as shown on its X-ray structure which clearly established the presence of two independent cationic trimethine cyanine motifs

linked by two C-C single bonds [101]. Such model allows to explain the particularly red-shifted absorption of this relatively simple molecule. The hypothesis of a “coupling principle” was experimentally demonstrated by Braunstein *et al.*, who investigated the acid-base properties of DABQDI **31a** which can be successively protonated twice to form the corresponding mono and dication, **31a·H⁺** and **31a·2H⁺** respectively, featuring two independent 6π-electrons systems on the same unsaturated cycle [93, 115]. X-ray analysis of crystals of monoprotonated specie **31a·H⁺** reveals the absence of bond length alternation between the nitrogen atoms of the trimethine unit (in the “upper part” of the molecule) whereas an alternation of single and double bonds could be observed between the nitrogen atoms of the lower part of the molecule. As expected, X-ray diffraction study of the diprotonated species **31a·2H⁺** revealed a full delocalization of the each 6π-subunits and the absence of conjugation between the two halves of the dyes. The red-shift of absorption measured in methanol/water solution going from **31a** (λ_{max} = 426 nm) to **31a·H⁺** (λ_{max} = 527 nm) and to **31a·2H⁺** (λ_{max} = 564 nm) is attributed to the π→π* intraquinone transition. Thus, this remarkable behavior is a rare example of acidochromy for which it is possible to control the degree of delocalization of two different π-subsystems in a single molecule depending on the pH. It is noteworthy that fluorescence is detectable for neutral quinone **31** when R = Ph (λ_{em} = 480 nm) and is dramatically quenched upon protonation of the system [115].

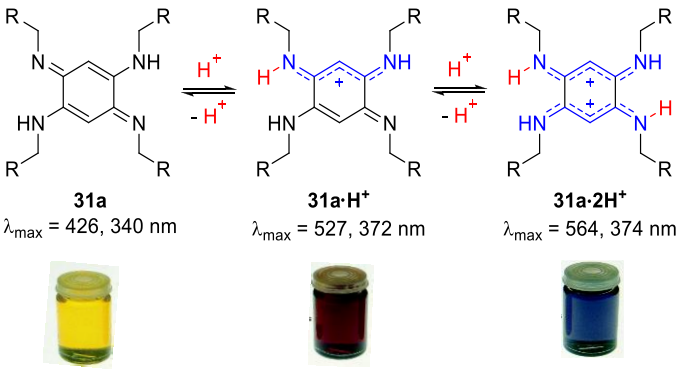

Scheme 17. Illustration of the coupling principle in 12-π electrons quinone **31a** (localized vs delocalized distribution upon protonation evidenced from X-ray analyses) and corresponding coloration in CH_2Cl_2 solution (R = ^{t}Bu) [93].

3.2.3. Redox properties

The deprotonation of DABQI ligand generally occurs during the formation of coordination complexes (see Section 4), generating $DABQDI^{2-}$ in which the two negative charges can be symmetrically delocalized between the trimethine units. This dianion can undergo two consecutive one-electron reductions to afford radical $DABQDI^{3-\bullet}$ then tetraanion $DABQDI^{4-}$ (Scheme 18). Consequently, these redox possibilities offers the opportunity to stabilize diamagnetic or paramagnetic species using this bridging ligand.

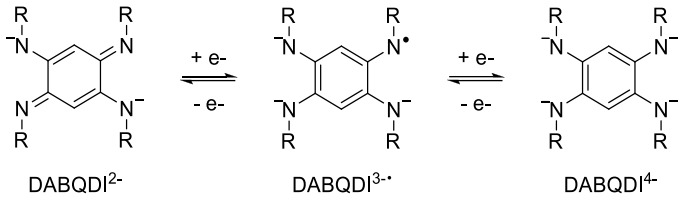

Scheme 18. Redox states of the deprotonated DABQDI ligand (adapted from ref. [116]).

In 2005, the redox versatility of DABQDI was further illustrated by oxidation of quinone **31** by AgOTf which lead to the formation of a red filtrate [117]. After electrochemical investigations, it turned out that following one-electron oxidation, two competitive pathways from **31**$^{+\bullet}$ tends to the generation dimer **32**, as the first example of reversible C-C coupling without dehydrogenation of a quinone derivative (Scheme 19).

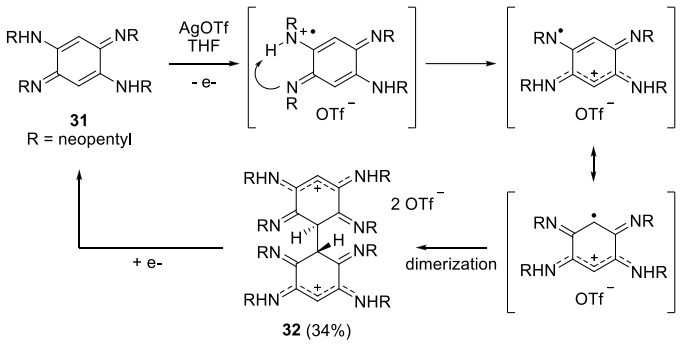

Scheme 19. Reversible dimerization of DABQDI [117].

4. Coordination chemistry of 2,5-diamino-*para*-benzoquinonediimines

4.1. Unsubstituted DABQDI ligand

Although 1,4-dihydroxybenzoquinone (DHBQ) is probably the most used quinoid ligand (more than 200 complexes based on mono-, dinuclear compounds, and polymers) [8], its stepwise metalation leading to dinuclear and oligomeric complexes has not been described to date. Surprisingly, the corresponding nitrogenated ligand DABQDI has been much less investigated since only two articles by Lever *et al.* in in 1993 and 2000, reported its use as ligand [68, 118]. In both cases, the DABQDI was prepared *in situ* in order to overcome its difficult isolation in good yield. Although the ruthenium complex **57** (Scheme 20) reported in 1993 was only characterized by NMR spectroscopy, this compound is - to the best of our knowledge - the first example of use of the unsubstituted 2,5-diamino-*p*-benzoquinonediimine (DABQDI) as ligand. In presence of base, TAB tetrachloride was converted into DABQDI, for which coordination to ruthenium was accompanied by an isomerization to the corresponding *ortho*-quinone. Complex **57** displays a weak low energy absorption band at 641 nm, which is dramatically red-shifted to 905 nm upon protonation of the ligand (**57·2H**$^{+}$), as the MLCT is reinforced.

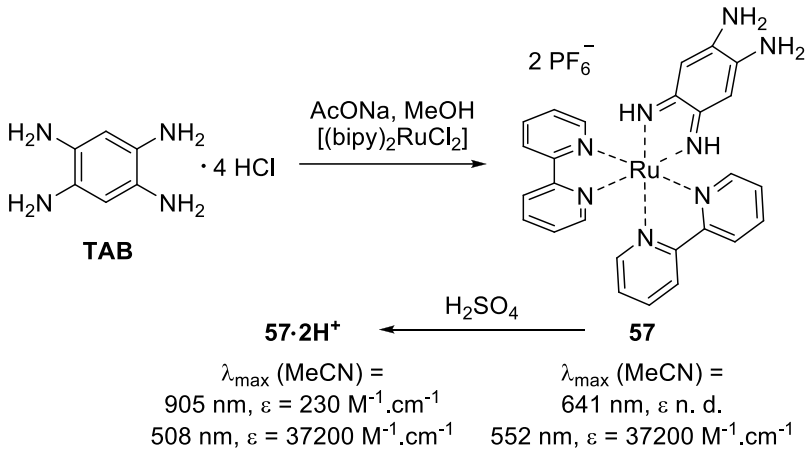

Scheme 20. Structure of Ru(II) complexes introducing an unsubstituted DABQDI ligand [68].

Upon treatment of TAB with $[Ru(bipy)_2(MeOH)_2]^{2+}$ (in presence of oxygen and water), the formation of a dinuclear Ru(II) complex **58** could be observed (Scheme 21) [118]. Surprisingly, during the course of the reaction, the expected bridging DABQDI ligand was converted to 1,2,4,5-tetraimino-3,6-diketocyclohexane, following a 1,4-Michael addition of two hydroxide molecules on an intermediate binuclear specie.

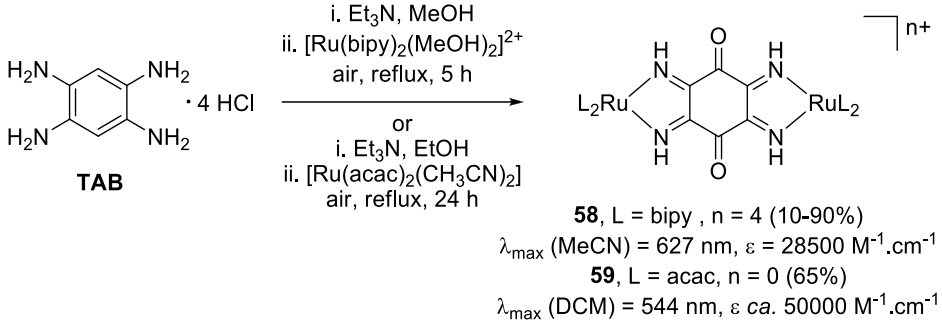

Scheme 21. Dinuclear Ru(II) complexes of 1,2,4,5-tetraimino-3,6-diketocyclohexane (bipy = 2,2'-bipyridine; acac = acetylacetonate) [118, 119].

The complex **58** exhibits strong absorption in the red region which is easily tune by electrochemical reduction of the ligand. Calculations and spectroelectrochemical measurements revealed a non-negligible mixing of the ruthenium orbitals through the bridging ligand, which increased upon reduction of the complex **58** to +3 (λ_{max} = 1176, 810 nm) and +2 (λ_{max} = 758 nm) oxidation states (Figure 6).

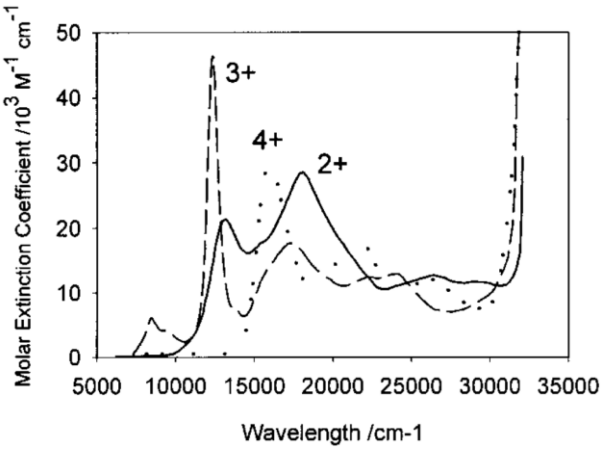

Figure 6. Absorption spectra of complex **58** and reduced forms *(ca.* 6.10^{-5} M) in acetonitrile containing 0.3 M Bu_4NPF_6 .Solid line: E = -0.27 V. Short-dashed line: E= 0.1 V. Long-dashed line: E = 0.55 V (potentials vs SCE). Reprinted with permission from Ref. [118]. Copyright 2000 American Chemical Society.

Lately, complex **59** featuring acetylacetonate ancillary ligands instead of bipyridines was prepared and shows intense and narrow absorption at 544 nm, assigned to a MLCT transition [119]. Compared to bipyridine, the acetylacetonate ligands favor the two consecutive metal-centered oxidations of **59** to the dicationic species $\mathbf{59^{2+}}$, which displays *ca.* 670 nm. Upon oxidation to $\mathbf{59^{+}}$, moderate mixed valence character implying Ru(II)/Ru(III) centers was identified by EPR (Figure 7), with *g* component splitting matching a lower Ru(III) species ($4d^5$ configuration), but however with no observation of IVCT band in the NIR. In contrast, upon reduction to $\mathbf{59^{-}}$, the MLCT transition is shifted to 628 nm and a weak band is noticed *ca.* 1040 nm (ε = 2200 $M^{-1}.cm^{-1}$), which, combined with EPR experiments showing broad signals at 298 and 110 K, suggests mixed orbital contributions from ligand and metal centers.

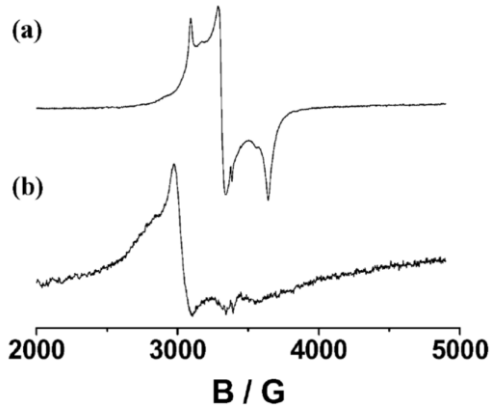

Figure 7. EPR spectra of (a) $\mathbf{59^{-}}$ and (b) $\mathbf{59^{+}}$ in dichloromethane (0.1 M Bu_4NPF_6) at 110 K with microwave frequencies of 9.4745 (a) and 9.4729 GHz (b), respectively. Reproduced from Ref. [119] with permission from The Royal Society of Chemistry.

So far, only one report deals with the direct metalation of unsubstituted DABQDI ligand that could successfully be isolated in a large scale in 2014 [78]. In presence of $Ni(acac)_2$, its metalation reaction easily form planar Ni-DABQDI tapes **60** which length depends on the solvent used for the reaction, the precipitation of the complex being the factor limiting the oligomerization process (Scheme 22).

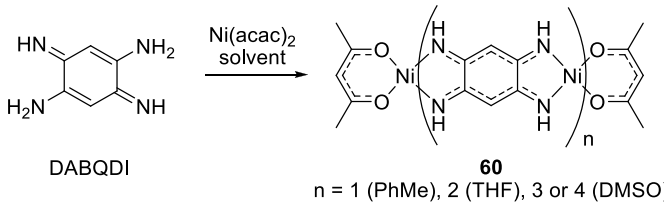

DABQDI

60

n = 1 (PhMe), 2 (THF), 3 or 4 (DMSO)

Scheme 22. Synthesis of Ni tapes of different lengths depending on the solvent (acac = acetylacetonate) [78].

Importantly, although theses complexes can be viewed as “extendable” since each oligomer can evolve in solution and rearrange into a longer form, they are also stable (that is, much more inert with respect to the oligomerization) depending on the solvent. In *N*,*N*-dimethylsulfoxide, the tetramer (*i.e.* the pentanuclear species) displays a broad absorption spamming from the UV up to 900 nm, in the NIR region (Figure 8). TD-DFT calculations pointed out that the red-shift which accompanied the oligomerization was mainly due to a very efficient extension of the effective conjugation pathway (Figure 8).

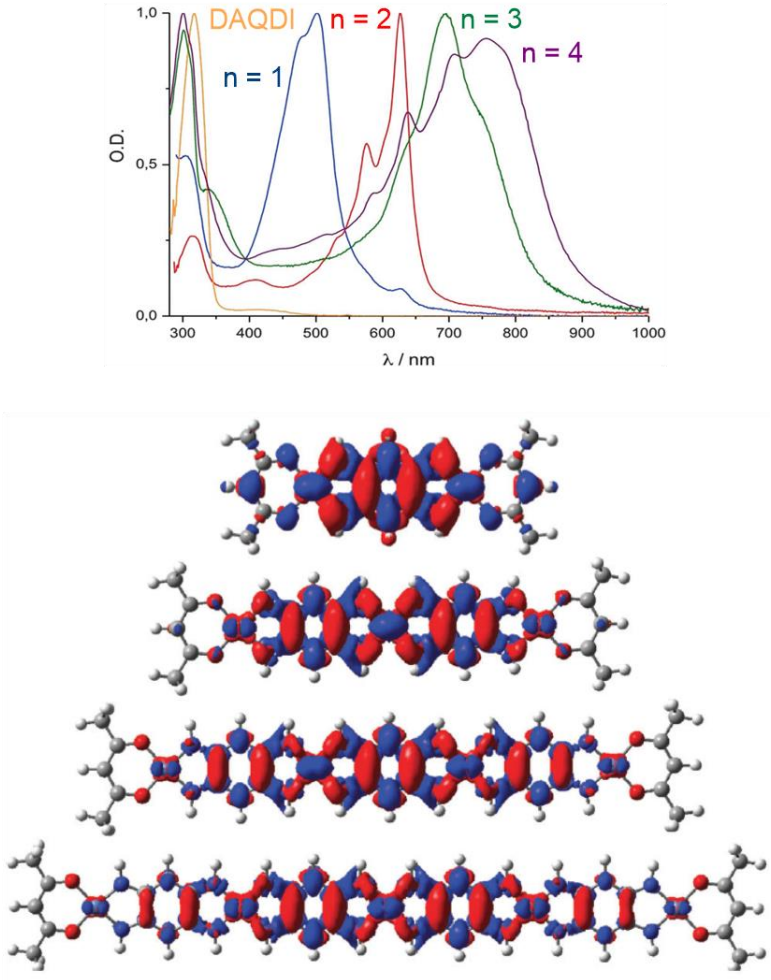

Figure 8. Absorption spectra (top) and M06/6-31G(d) delta density plots (bottom) between the excited and ground states for Ni tapes **60** of different lengths. Red (blue) regions indicate increase (decrease) of the density upon absorption [78]. Reproduced by permission of The Royal Society of Chemistry.

4.2. *N*-substituted DABQDI ligand

Complexes based on *C*-substituted QDIs are hitherto unknown but it is relevant to mention that *N*-substituted DABQDI ligands have attracted much more interest compared to unsubstituted DABQDI, as their easy access and high solubility paved the way to their use in the preparation of mononuclear and dinuclear complexes.

4.2.1. Mononuclear complexes

Kaim and co-worker reported in 1998 that the treatment of azophenine with one or two equivalents of $[Cu(PPh_3)_4][BF_4]$ leads in both cases to the formation of a mononuclear complex **61** (Chart 4) [120]. After crystallization of the specie, it was first observed that the original 1,4-quinone isomerized to a 1,2-quinone during chelation to Cu(I). A second interesting feature was the presence of an interaction between a fluorine atom of the BF_4 ion and the pendant N-H hydrogens of the *o*-diamine part of the ligand, thus explaining the stability of the complex. A metal-induced tautomerism was also evidenced to take place during the coordination of azophenine to $[Re(CO)_5Cl]$ complex [121]. In this instance, additional stabilization of the mononuclear complex **62** was brought in the solid state by Cl···H interactions between the N-H hydrogens of the *ortho*-diamino motif and the chlorine atom of a neighbor complex. UV-Vis absorption of the copper (**61**) and rhenium (**62**) complexes shows broad absorptions spamming from the UV up to 700 nm with high extinction coefficients and the low energy bands were attributed to MLCT transitions. Interestingly, tungsten analogs **63a-b** reported by Braunstein *et al*. in 2004 revealed no need of stabilization by H-bonding interactions. These W(0) complexes display absorption centered in the red region and allow to evidence a possible tuning of the absorption maxima by variation of the nitrogen substituents [122]. More recently, reaction of the DABQDI ligand with $Ni(ClO_4)_2$ hexahydrate in DCM provided the Δ and Λ enantiomers of mononuclear complex **64**, the Ni(II) center adopting a distorted octahedral geometry. The bond length analysis disclosed the new electronic distribution within the 4,5-diamino-*o*-BQDI ligand, which implies that metal-induced tautomerism occurs during formation of the complex [123].

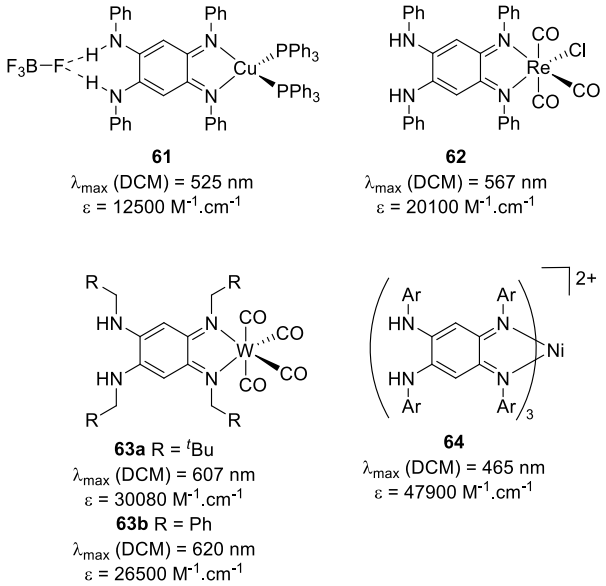

Chart 4. Monometallic complexes introducing an isomerized 4,5-diamino-*o*-BQDI [120-123].

4.2.2. Dinuclear complexes

4.2.2.1. Dinuclear complexes from aromatic TAB

The first attempts to generate dinuclear complexes resulted from deprotonation and oxidation of *N*-substituted tetramethylsulfonyl-1,2,4,5-tetraaminobenzene ligand **65**, described by Peng *et al.* in 1992 [124]. Interestingly, the X-ray structures of the dinuclear Cu(I) complex **66a** exhibited non-alternant bond lengths within the N-C1-C2-C3-N bridges and particularly long bonds between C1-C1' and C3-C3' (Scheme 23). These data confirmed that oxidation of the TAB precursor occurs during the coordination reaction, generating a non-aromatic DABQDI-type ligand.

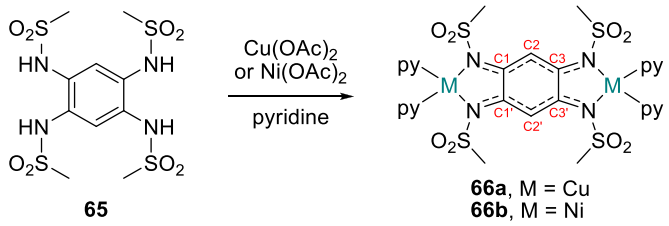

Scheme 23. Cu(I) and Ni(II) complexes of *N*,*N*′,*N*″,*N*‴-tetramethylsulfonyl-DABQDI (py = pyridine) [124].

In their attempts to prepare new ditopic carbenes, Hahn *et al.* investigated the formation of *N*-heterocycles from a tetrasubstituted TAB [125]. While, on the one hand, the reaction of **69** with $Ge[N(SiMe_3)_2]_2$ leads to the formation of the expected benzo bisgermylene complex **70**, the reaction with $Se[N(SiMe_3)_2]_2$ in presence of oxygen triggered on the other hand the oxidation of the TAB to the corresponding DABQDI and the bisstannylene **71** was isolated as a red-purple compound (Scheme 24). Molecular structure of **71** displayed the typical bond lengths corresponding to a 6π + 6π bridging DABQDI unit (*vide supra*) and assed the electronic delocalization within the stannylene heterocycles.

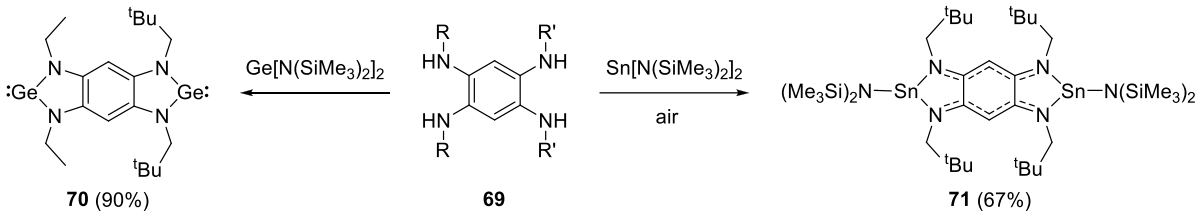

70 (90%) **69** **71** (67%)

Scheme 24. Preparation of benzobisgermylene and quinobisstannylene [125].

Using their tetrakis(tetramethylguanidino)benzene precursor **47** (Scheme 13), Himmel and co-workers reported several examples of polynuclear complexes for which the bridging ligand adopted aromatic (Zn(II), Cu(I), Pt(II)) or quinoidal structures (Cu(II)) and properly characterized most of them by means of X-ray diffraction [126]. Among them, hexacationic complex **72** was identified in 2009 as the first example of dinuclear Cu(II) bridged by a tertiary amine-containing DABQDI derivative (Scheme 25). A antiferromagnetic coupling was evidenced between the two Cu(II) centers with J = -35.4 cm^{-1}. In a prolongation of these works, the authors demonstrated the possibility to prepare neutral, monocationic and dicationic (**73**) analogues by slight modifications of the reaction parameters [127]. In the case of **73**, a weak antiferromagnetic coupling between the Cu(II) was evidenced. However, a strong ferromagnetic coupling was additionally measured between the radical cation bridging-ligand and the metallic extremities in the case of the cationic analogue.

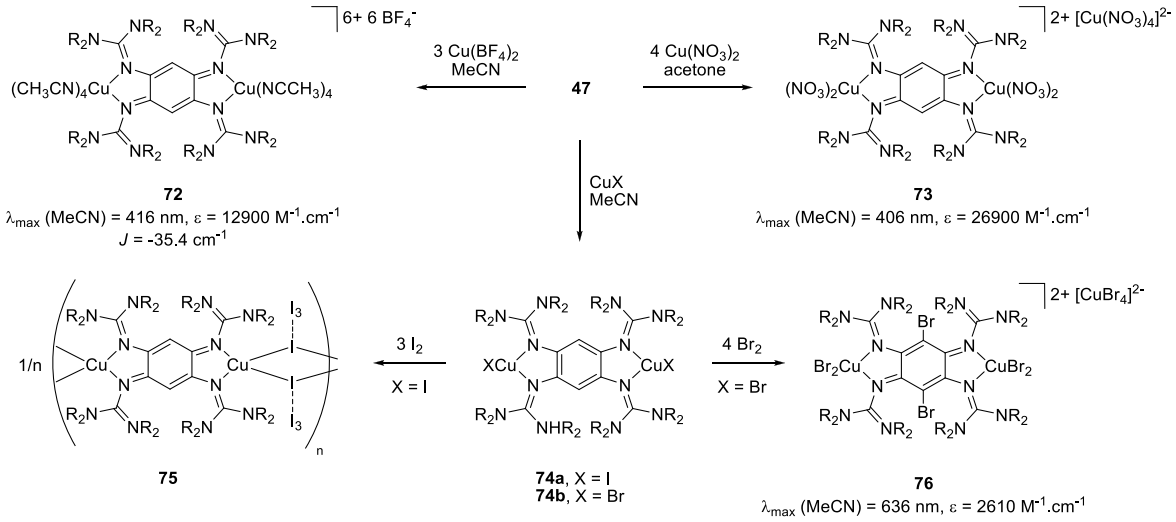

72
λ_{max} (MeCN) = 416 nm, ε = 12900 M^{-1}.cm^{-1}
J = -35.4 cm^{-1}

47

73
λ_{max} (MeCN) = 406 nm, ε = 26900 M^{-1}.cm^{-1}

75

74a, X = I
74b, X = Br

76
λ_{max} (MeCN) = 636 nm, ε = 2610 M^{-1}.cm^{-1}

Scheme 25. Polynuclear complexes from a tetrakis(tetramethylguanidino)benzene precursor [126-128].

Starting from a Cu(I) complex bridged by an aromatic ligand (**74a**), oxidation in presence of iodine led to the formation of a polymeric complex **75** [128]. The authors suggested that the unusual structure of this polynuclear complex, notably the Cu(μI)$_2$Cu unit, could be preferred because of I···I interaction. Semi-conductor properties have been evidenced for black polymer **75**, with an estimated band gap of 1.05 eV. Interestingly, the treatment of **74b** with bromine led to the oxidation of the complex to form the Cu(II) dinuclear specie **76** and the reaction was accompanied by a substitution of the central ligand with Br atoms. Thereafter, analogue of **75** has been developed starting from a 2,3,5,6-tetrakis(tetramethylguanidino)pyridine [129]. Moreover, a green Ag(I) polymer obtained from **47** was identified as a semi-conductor with an estimated band gap *ca.* 3 eV [130].

4.2.2.2. Dinuclear complexes from *N*-substituted DABQDI

The first metalation reaction of DABQDI affording the corresponding dinuclear complex was reported in 2000 by Braunstein and Siri [92]. A dinuclear Pt(II) complex incorporating a DABQDI bridging unit (**78**, Scheme 26) was obtained by reaction of **31a** with 2 equivalents of [$PtCl_2$(COD)] in basic conditions. X-ray analysis evidenced the square planar geometry of the metal centers and the bond length analysis revealed a totally delocalized π-structure between the two trimethine units, linked by two longer single C-C bonds (1.53 Å). Moreover, it also revealed an evolution of the cyclooctadienyl (COD) ligand during the course of the metalation reaction. Dicationic intermediate complex **77** (not isolated) underwent a deprotonation of the COD moiety in presence of trimethylamine, leading to **78** with both (1,2-η^2-6-σ-cycloocta-1,4-dienyl) ligands being σ,π-bonded to the metal centers [131]. The main absorption band of **78** centered at 504 nm is attributed to a MLCT transition, while a characteristic π→π* intraquinone CT is observed at 479 nm.

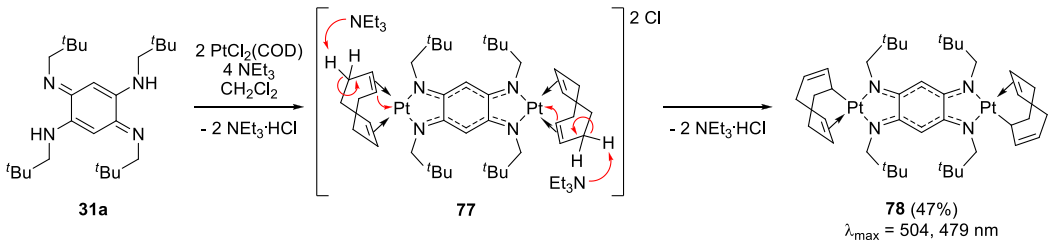

Scheme 26. Mechanism of formation of dinuclear Pt(II) complex [92, 131].

Metalation of DABQDI ligands with $M(acac)_2$ could be also successfully carried out affording dinuclear species with metal centers and *N*-substituents of different nature (Scheme 27). Ni(II) and Pd(II) complexes **79a-c** and **80a-b** exhibit similar electronic structures with two 6π-electron subsystems allowing a high delocalization between the two metals (see bond length on Figure 9) [131, 132]. The series **79a-d** allows for a comparison of the influence of the *N*-substituents on the electronic absorption of the Ni(II) complexes. A red-shift from 510 to 555 nm is observed going from neopentyl to phenyl substituents. However, this tendency is surprisingly not observed in the case of Pd(II) analogues **80a-b**, these complexes showing absorption centered *ca.* 490 nm. Cyclic voltammetry of **79a** shows two reversible one electron oxidations at 0.05 and 0.91 V *vs.* Fc^+/Fc and higher potentials for more electron poor **79b**. Intriguingly, upon oxidation of **79a**, appearance of two bands at 1030 and 910 nm was noticed [132]. Theoretical calculations pointed out that the oxidation was mainly related to the bridging quinone unit. However, in presence of additional pyridine, EPR analysis of **79a**$^+$ at 4 K exhibited two broad signals (g = 2.13 and 4.16), which revealed a ferromagnetic coupling between Ni(III) and Ni(II) centers, the formed specie being therefore a mixed-valence complex of class III [133].

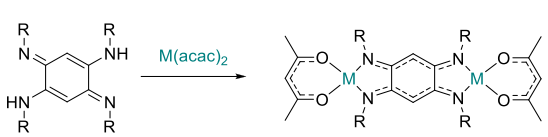

79a, M = Ni, R = $CH_2{}^tBu$ (55%) λ_{max} (DCM) = 510 nm, ε = 14800 $M^{-1}.cm^{-1}$
79b, M = Ni, R = CH_2Ph (76%) λ_{max} (DCM) = 519 nm, ε = 34700 $M^{-1}.cm^{-1}$
79c, M = Ni, R = Ph (82%) λ_{max} (DCM) = 555 nm, ε = 19500 $M^{-1}.cm^{-1}$
79d, M = Ni, R = *p*-Et-Ph (64%) λ_{max} (DCM) = 559 nm, ε = 52500 $M^{-1}.cm^{-1}$

80a, M = Pd, R = $CH_2{}^tBu$ (55%) λ_{max} (DCM) = 491 nm, ε = 66100 $M^{-1}.cm^{-1}$
80b, M = Pd, R = CH_2Ph (49%) λ_{max} (DCM) = 488 nm, ε = 10000 $M^{-1}.cm^{-1}$

Scheme 27. Structure of dinuclear Ni(II) and Pd(II) complexes incorporating a DABQDI bridge [123, 131, 132].

It is worth mentioning that complex **79a** has been evaluated as candidate pre-catalyst for the oligomerization of ethylene [131]. In presence of diethylaluminium chloride co-catalyst, the complex showed moderate activity but high selectivity for the production of C_4 and C_6 olefins. Afterwards, an azophenine Ni(acac) dinuclear complex has been successfully used as efficient catalyst for the polymerization of norbornene and methyl methacrylate [134]. In 2015, the dinuclear complex **79d** has been used for the polymerization of styrene and the engineering of the bulky *N*-susbtituents provided efficient pre-catalysts [97].

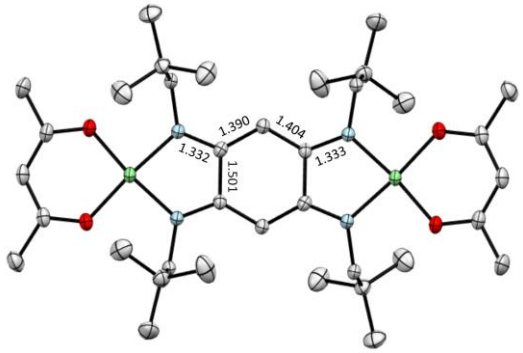

Figure 9. Structure and selected bond lengths (Å) of complex **79a** [132]; Anisotropic displacement parameters at 50%; H atoms are omitted for clarity.

Works reported by Fujihara *et al.* described the preparation of the B(III) dinuclear complex **82** by deprotonation of the appropriate ligand **81** with butyllithium followed by chelation to BF_3•OEt_2 (Chart 5) [123]. This complex exhibits bond order similar to the free diprotonated ligand (*i.e.* two independent 6π-electron systems), with however an absorption located at the edge of the UV-Vis region (λ_{max} = 447 nm). The deprotonated ligand was mixed with $[(Ir(Cp^*)Cl)_2Cl_2]$ to prepare the first example of dinuclear Ir(III) complex bridged by a DABQDI ligand (**83**). This complex exhibits two highly delocalized π-electron subunits and an intense absorption in the same range that the Ni(II) analogue **79d** (Scheme 27).

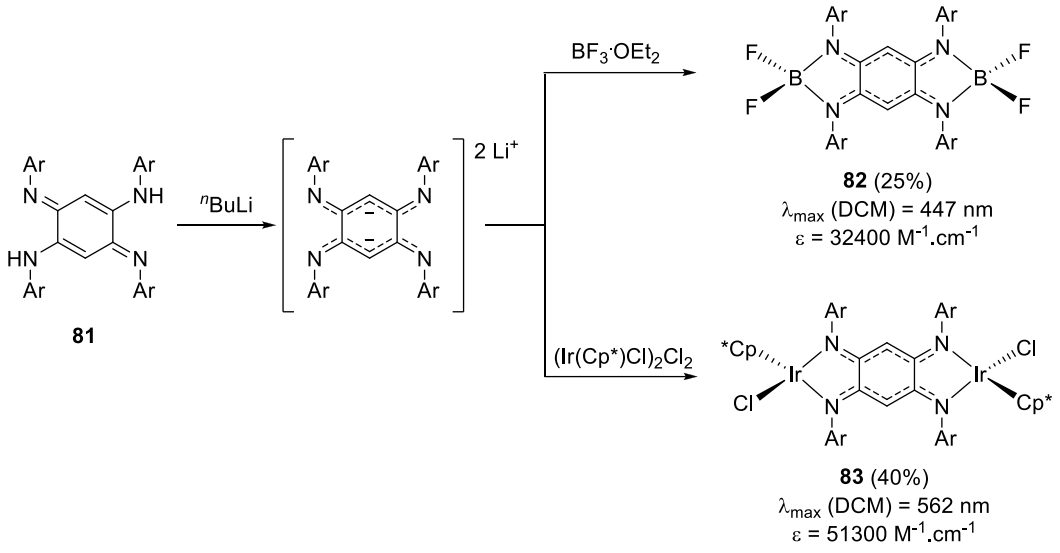

Chart 5. B(III) and Ir(III) complexes of DABQDI [123] (Ar = *p*-Et-Ph; Cp* = pentamethylcyclopentadienyl).

Yang and collaborators reported in 2012 the first complexes of DABQDI chelated to alkali metals, **85-86**, presented in Scheme 28 [135]. In presence of two equivalents of ^{n}BuLi, quinone **84** yielded the dinuclear specie **85**, the two lithium atoms being distorted tetrahedral and slightly out of the plane of the two chelating nitrogen atoms. In contrast, the ligand underwent polymerization in presence of sodium in 1,2-dimethoxyethane. The structure of **86** displays similarities with its Li analogue, with two chemically linked 6π-electron subunits, but however, in this case, a higher coordination number of the alkali metal. Salt metathesis using $ZnCl_2$ was efficiently performed on complex **85** and polymer **86** to afford the corresponding tetranuclear units **87** and **88**, respectively. The authors mention the red to purple color changes for the compounds they characterized, but unfortunately this work does not give any information about the absorption or redox properties of these original complexes.

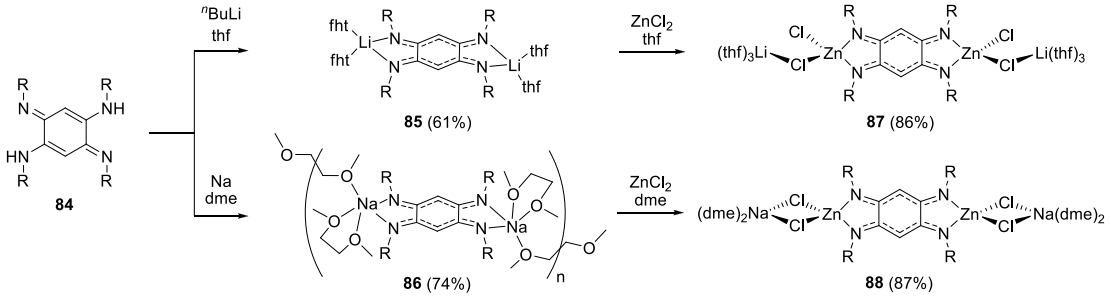

Scheme 28. Alkali metal-containing DABQDI complexes (R = 2,6-^{i}Pr$_2$-C$_6$H$_3$; thf = tetrahydrofuran; dme = 1,2-dimethoxyethane) [135].

In 2013, Sarkar and co-workers reported a series of bridged dinuclear complexes of Cu(II) introducing deprotonated DHBQ [O,O,O,O], 2,5-dianilino-1,4-benzoquinone [O,NAr,O,NAr] or azophenine **27** [NPh,NPh,NPh,NPh] ligands to investigate their electrochemical and magnetic properties [136]. Interestingly, while the oxo-ligand-based complexes showed a distorted octahedral environment around the metal, the Cu(II) centres in derivative **89** (Figure 10) adopted distorted square-pyramidal coordination geometries. Susceptometry measurement using a superconducting quantum interference device (SQUID) revealed a high intramolecular coupling between the two copper atoms,

with an isotropic exchange coupling constant J = -23.2 cm^{-1}. TD-DFT calculations pointed out that this larger value was mainly related to the superior polarizability and the elevated proportion of total spin density held by the N donor atoms of the ligand. A high exchange coupling constant is particularly relevant for the development of single molecule magnets since it guarantees a larger separation between spin ground and excited states, thus preventing fast relaxation of the magnetization [9].

The redox properties of **89** could not be screened because of the poor stability of the complex. However spectroelectrochemistry has been investigated in the case of a dinuclear Pt(II)-azophenine complex **3.35** featuring peripheral azobenzene ligands [137]. Complex **90** possesses an irreversible oxidation and three reversible reductions in THF which have a major influence on the electronic absorption (Figure 10). The neutral specie exhibits an absorption maximum at 619 nm which is red-shifted to 770 nm upon one-electron reduction and accompanied by the appearance of a particularly broad band centred *ca.* 1870 nm. Second and third reduction of **90** lead to a dramatic decrease of the lowest energy band and intense absorption at 1351 and 1191 nm, respectively.

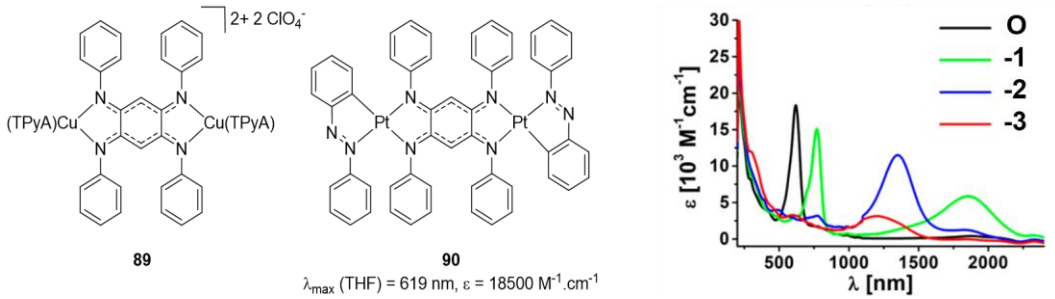

Figure 10. Azophenine-based dinuclear complexes **89-90** [136, 137] and absorption spectra of **90** under various redox states (TPyA = tris(2-pyridylmethyl)amine). Reprinted with permission from ref. [137]. Copyright 2014 American Chemical Society.

In the continuity of the promising magnetic assets measured on **89**, Harris and co-workers prepared and crystallized from azophenine the analogous dicationic complex **91** containing two Fe(II) centers and the corresponding reduced cationic species **92** (Figure 11) [116]. Analysis of the bond lengths of the ligand showed once again high conjugation within the N-C-CH-C-N fragments for both complexes, with a noticeable decrease of the N-Fe bonds length in the reduced specie, testifying of a stronger ligand-metal interaction. Mössbauer spectroscopy confirmed that the first reduction occurred on the deprotonated azophenine ligand, thus noted as $DABQDI^{3-\bullet}$, which explained its highest affinity for the Fe(II) centers. The investigation of the magnetic properties of **91** revealed a weak exchange coupling between the two ionic centers (J = -2.90 cm^{-1}). However for the reduced specie **92**, the J constant was estimated to the order of 900 cm^{-1}, a record value which attests of a strong antiferromagnetic exchange between the radical ligand and the iron atoms.

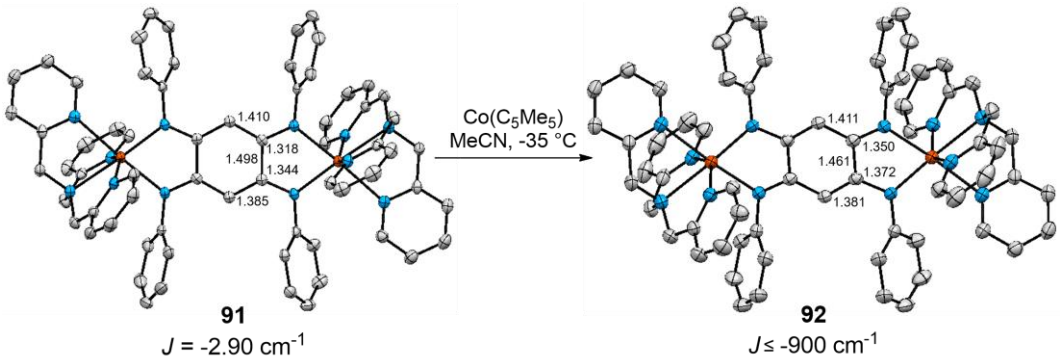

Figure 11. Structure and selected bond lengths (Å) of dinuclear Fe(II) complex **91** and its reduced form **92** [116]; Anisotropic displacement parameters at 50%; H atoms and counter-ions are omitted for clarity.

Lately, Harris and collaborators repeated the study on a series of dinuclear complexes of Cr(III), Mn(II), Fe(II) and Co(II) and using a slightly bulkier tetramethyl azophenine derivative (L, Figure 12) [138]. The voltamogramms of the series are mainly characterized by one and three reversible one-electron reductions for **94-96** and **93**, respectively. The weak variation of reduction potentials, from -1.93 V (**94**) to 1.68 V (**96**) is consistent with an azophenine ligand-centered process. In the case of **93**, azophenine reduction occurs at -0.50 V, and the two additional processes beyond -1.50 V are attributed to Cr(III) reduction to Cr(II). Once the one-electron reduction occurred on the deprotonated ligand, impressive values of exchange coupling constants were determined, up to -626 cm^{-1} for the Cr(II) complex **97**. It is noteworthy that the steric bulk brought by the additional methyl on the phenyl rings is probably to account regarding the three-fold lower *J* value for **99** (*J* = -307 cm^{-1}) compared to **92**. The M-N bond distance between the ligand nitrogen and the metal within **93-96** can be linearly correlated to the radical exchange constant of **97-100**, the lower distances in the reduced species giving rise to the higher *J* values for the oxidized complexes.

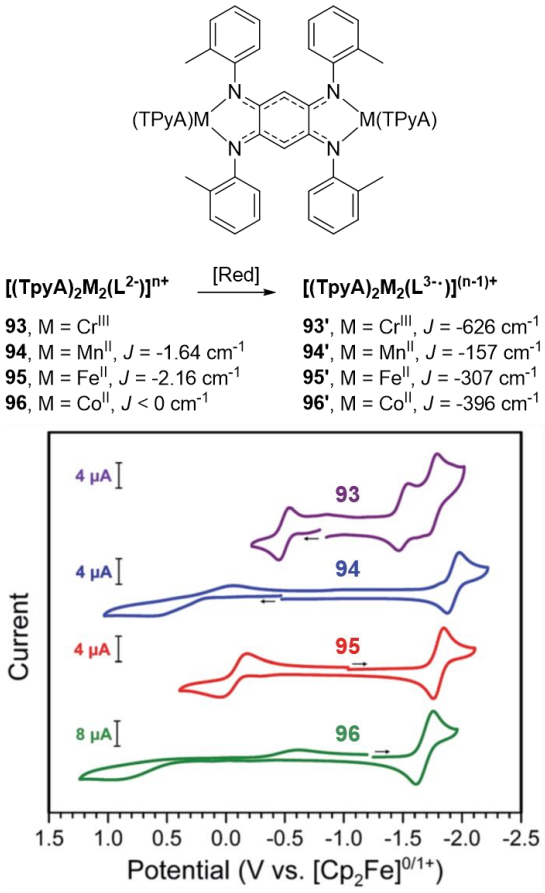

Figure 12. Efficient dinuclear single-molecule magnets developed by Harris *et al*. and cyclic voltammograms (v = 0.1 V.s^{-1}) for solutions of **93** (MeCN), **94** (THF), **95** (THF) and **96** (THF). Adapted from Ref. [138]. Published by The Royal Society of Chemistry.

4.2.3. Tetranuclear complexes

Siri, Braunstein and co-workers highlighted a drastic ancillary ligand effect that occurred by replacing the [Pd(acac)$_2$] reagent with [Pd(OAc)$_2$]. Whereas the metalation of DABQDI **31a** with [Pd(acac)$_2$] led to the formation of a dinuclear complex **80a** (Scheme 27), the use of [Pd(OAc)$_2$] afforded instead a tetranuclear Pd(II) complex **101** (Figure 13) [139]. While NMR analysis revealed a high symmetry complex, X-ray diffraction allowed to conclude that the structure was highly stabilized by the π-stacking of the two benzoquinone units (3.80 Å). The absorption of the tetranuclear species is characterized by a band centered at 428 nm, which is blue-shifted compared to the dinuclear complex **80a** (λ_{max} = 491 nm). Two successive one-electron oxidations lead to the **101**$^{+}$ and **101**$^{2+}$ species (resp. 0.45 and 0.77 V *vs.* SCE), and a third oxidation was reached at higher potentials (1.50 V *vs.* SCE). Unfortunately, the fourth oxidation of the dimer could not be observed due to the oxidation of the electrolyte.

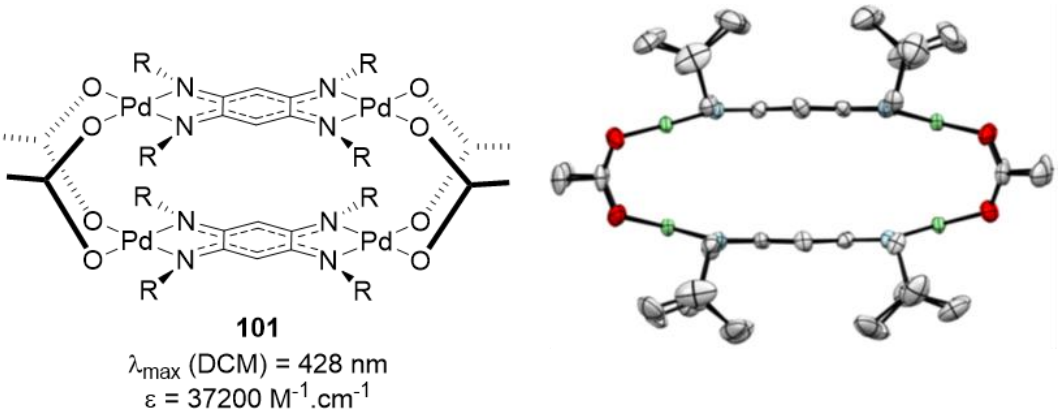

Figure 13. Tetranuclear Pd(II) complex **101** and side-view of its structure (R = $CH_2{}^tBu$) [139]; Anisotropic displacement parameters at 50%.

5. Conclusion

2,5-diamino-1,4-benzoquinonediimines (DABQDI) can be considered as an emerging class of promising ligands in coordination chemistry whereas their first preparation was reported more than a century ago (Figure 14). The first member - *N*-substituted with phenyl groups (azophenine) – was discovered by Kimich in 1875 through self-condensation of aniline. Few years later (1887), the unsubstituted parent molecule was reported by Nietzki when he observed the unstability of 1,2,4,5-tetraaminobenzene (TAB) under air. Then, this type of N_4 ligands was (surprisingly) not investigated during more than a century, whereas its oxygenated analogue O_4 was the object of numerous studies in coordination chemistry. If Lever *et al.* mentioned the possible isomerization of DABQDI upon metalation in 1993, Kaim *et al.* was the first to fully characterize a (mononuclear) complex in 1998. From 2000, year in which Braunstein published the first *N*-alkylated ligand and its dinuclear complex [Pt(II)], the coordination chemistry of these *N*-substituted ligands attracted the interest of a large scientific community for the synthesis of complexes with unusual properties (M = Ru, Fe, Cu, Pd, Ni, Zn, Ir, Sn, W, Re, Na, Li, B).

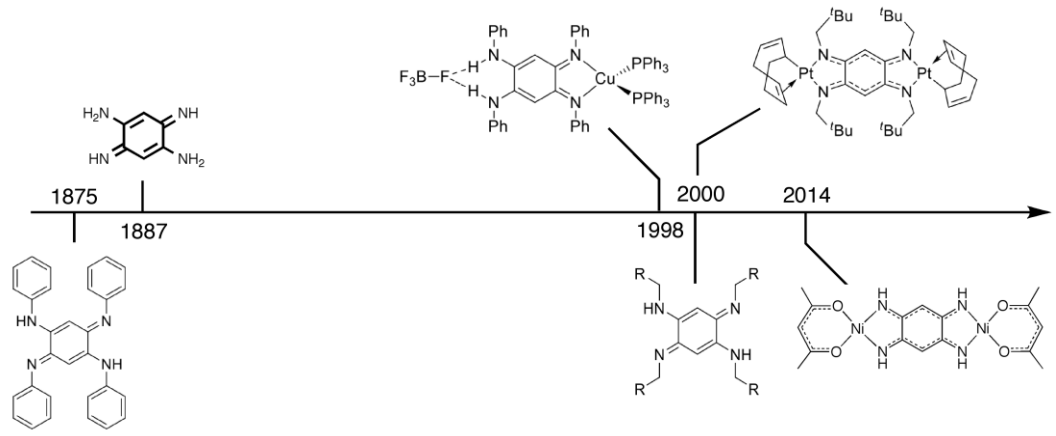

Figure 14. Timeline of BQMIs synthesis and use as ligand.

In 2014, our group reported the first direct metalation of unsubstituted DBQDI (127 years after its first report), revealing a drastic different behavior by comparison with the *N*-substituted analogues. Because of its possible isomerization process upon coordination, 2,5-diamino-1,4-benzoquinonediimines (DABQDI) can be viewed as a ligand that combines the structural elements of *ortho*- and *para*-benzoquinonediimines (*o*-BQDI and *p*-BQDI) which are bidentate monotopic and monodentade ditopic ligands, respectively. These two classes of BQDI ligands have been also reviewed in order to parallel their properties to those of the complexes based on DABQDI depending on the metal center(s). For instance, the well-known non-innocent, *i.e.* redox active, *o*-BQDI ligands – which play a crucial role in the complexes depending on the degree of π-backdonation – might be used as model for understanding the properties of the mononuclear compounds based on *o*-DABQDI. Similarly, *p*-BQDI bridging ligands can be viewed as model compounds for highlighting the influence of two 6π-subunits in DABQDI ligands in the metal-metal interactions of the dinuclear complexes (*i.e.* two conjugated pathways for DABQDI instead of one in *p*-BQDI).

In summary, 2,5-diamino-1,4-benzoquinonediimine (DABQDI) offers important possibilities into coordination chemistry because of 1) the presence of *N*-substituents that can be so far tuned almost at will, and 2) the easy introduction of metal centers of different nature depending on the targeted application. Reports on the use of these ligands are seldom described and mainly focused on few examples among others 12π-electrons quinones. This review report in details the synthesis and coordination chemistry of DABQDI ligands with the hope to highlight their exceptional versatility and to stimulate researchers to extend the use of these ligands and their corresponding complexes to embrace new discoveries.

AKNOWLEDGEMENTS

This work was supported by the CNRS and the Ministère de la Recherche (Paris). The authors wish to thank all the contributions cited in this review for the development of the quinonediimine chemistry. O. S. expresses his warmest thanks to Pierre Braunstein for the five wonderful years spent working together.

REFERENCES

[1] E.R. Brown, Quinonediimines, monoimines and related compounds, in: The Quinonoid Compounds (1988), John Wiley & Sons, Inc., 2010, pp. 1231-1292.
[2] S. Hünig, Pure Appl. Chem., 62 (1990) 395-406.
[3] J. Moussa, H. Amouri, Angew. Chem. Int. Ed., 47 (2008) 1372-1380.
[4] J. Casado, R. Ponce Ortiz, J.T. Lopez Navarrete, Chem. Soc. Rev., 41 (2012) 5672-5686.
[5] C. Asche, Mini-Rev. Med. Chem., 5 (2005) 449-467.
[6] J. López, F. de la Cruz, Y. Alcaraz, F. Delgado, M.A. Vázquez, Med. Chem. Res., 24 (2015) 3599-3620.
[7] M.D. Ward, Chem. Soc. Rev., 24 (1995) 121-134.
[8] S. Kitagawa, S. Kawata, Coord. Chem. Rev., 224 (2002) 11-34.
[9] S. Demir, I.-R. Jeon, J.R. Long, T.D. Harris, Coord. Chem. Rev., 289–290 (2015) 149-176.
[10] B. Sarkar, D. Schweinfurth, N. Deibel, F. Weisser, Coord. Chem. Rev., 293–294 (2015) 250-262.
[11] J.L. Boyer, J. Rochford, M.-K. Tsai, J.T. Muckerman, E. Fujita, Coord. Chem. Rev., 254 (2010) 309-330.
[12] V. Lyaskovskyy, B. de Bruin, ACS Catalysis, 2 (2012) 270-279.

[13] O.R. Luca, R.H. Crabtree, Chem. Soc. Rev., 42 (2013) 1440-1459.
[14] W. Kaim, G.K. Lahiri, Angew. Chem. Int. Ed., 46 (2007) 1778-1796; and references therein.
[15] O.J.X. Morel, R.M. Christie, Chem. Rev., 111 (2011) 2537-2561.
[16] A. Meyer, K. Fischer, Environ. Sci. Europe, 27 (2015) 11.
[17] H. Berneth, Azine Dyes, in: Ullmann's Encyclopedia of Industrial Chemistry, Wiley-VCH Verlag GmbH & Co. KGaA, 2000.
[18] R.E. Smith, S. Updated by, Azine Dyes, in: Kirk-Othmer Encyclopedia of Chemical Technology, John Wiley & Sons, Inc., 2000.
[19] C. Seillan, H. Brisset, O. Siri, Org. Lett., 10 (2008) 4013-4016.
[20] Q. Tang, J. Liu, H.S. Chan, Q. Miao, Chem. Eur. J., 15 (2009) 3965-3969.
[21] S.K. Roy, S. Samanta, M. Sinan, P. Ghosh, S. Goswami, J. Org. Chem., 77 (2012) 10249-10259.
[22] U.H.F. Bunz, J.U. Engelhart, Chem. Eur. J., 22 (2016) 4680-4689.
[23] S. Banerjee, ARKIVOC, 2016 (2016) 82-110.
[24] J. Li, S. Chen, Z. Wang, Q. Zhang, Chem. Rec., 16 (2016) 1518-1530.
[25] P.-Y. Gu, Z. Wang, Q. Zhang, J. Mater. Chem. B, 4 (2016) 7060-7074.
[26] K. Rieder, U. Hauser, H. Siegenthaler, E. Schmidt, A. Ludi, Inorg. Chem., 14 (1975) 1902-1907.
[27] S. Joss, P. Bigler, A. Ludi, Inorg. Chem., 24 (1985) 3487-3488.
[28] S. Joss, H. Reust, A. Ludi, J. Am. Chem. Soc., 103 (1981) 981-982.
[29] S. Joss, H.B. Buergi, A. Ludi, Inorg. Chem., 24 (1985) 949-954.
[30] E.F.G. Herington, J. Chem. Soc., (1959) 3633.
[31] E.H. Cutín, N.E. Katz, P.A.M. Williams, P.J. Aymonino, Trans. Met. Chem., 16 (1991) 155-159.
[32] Y. Wei, C. Yang, T. Ding, Tetrahedron Lett., 37 (1996) 731-734.
[33] T. Moriuchi, T. Hirao, Acc. Chem. Res., 45 (2012) 347-360.
[34] T. Moriuchi, S. Bandoh, M. Miyaishi, T. Hirao, Eur. J. Inorg. Chem., 2001 (2001) 651-657.
[35] T. Moriuchi, M. Miyaishi, T. Hirao, Angew. Chem. Int. Ed., 40 (2001) 3042-3045.
[36] L.A.P. Kane-Maguire, G.G. Wallace, Chem. Soc. Rev., 39 (2010) 2545-2576.
[37] X. Shen, T. Moriuchi, T. Hirao, Tetrahedron Lett., 45 (2004) 4733-4736.
[38] T. Moriuchi, X. Shen, T. Hirao, Tetrahedron, 62 (2006) 12237-12246.
[39] T. Hirao, S. Fukuhara, Y. Otomaru, T. Moriuchi, Synth. Met., 123 (2001) 373-376.
[40] T. Hirao, K. Iida, Chem. Commun., (2001) 431-432.
[41] X. Shen, T. Moriuchi, T. Hirao, Tetrahedron Lett., 44 (2003) 7711-7714.
[42] T. Moriuchi, J. Shiori, T. Hirao, Tetrahedron Lett., 48 (2007) 5970-5972.
[43] T. Moriuchi, X. Shen, K. Saito, S. Bandoh, T. Hirao, Bull. Chem. Soc. Jpn., 76 (2003) 595-599.
[44] T. Moriuchi, Y. Takagi, T. Hirao, Eur. J. Inorg. Chem., 2008 (2008) 3877-3882.
[45] A.B.P. Lever, H. Masui, R.A. Metcalfe, D.J. Stufkens, E.S. Dodsworth, P.R. Auburn, Coord. Chem. Rev., 125 (1993) 317-331.
[46] A. Mederos, S. Domínguez, R. Hernández-Molina, J.N. Sanchiz, F. Brito, Coord. Chem. Rev., 193–195 (1999) 913-939.
[47] K.P. Butin, E.K. Beloglazkina, N.V. Zyk, Russ. Chem. Rev., 74 (2005) 531.
[48] A.B.P. Lever, Coord. Chem. Rev., 254 (2010) 1397-1405.
[49] H.-L. Chan, H.-Q. Liu, B.-C. Tzeng, Y.-S. You, S.-M. Peng, M. Yang, C.-M. Che, Inorg. Chem., 41 (2002) 3161-3171.
[50] T. Bugarcic, A. Habtemariam, R.J. Deeth, F.P.A. Fabbiani, S. Parsons, P.J. Sadler, Inorg. Chem., 48 (2009) 9444-9453.
[51] S. Taheri, M. Behzad, H. Nazari, A. Khaleghian, ISRN Inorg. Chem., 2013 (2013) 6.
[52] F. Feigl, M. Fürth, Monatsh. Chem., 48 (1927) 445-450.
[53] E.I. Stiefel, J.H. Waters, E. Billig, H.B. Gray, J. Am. Chem. Soc., 87 (1965) 3016-3017.
[54] A.L. Balch, F. Röhrscheid, R.H. Holm, J. Am. Chem. Soc., 87 (1965) 2301-2302.
[55] A.L. Balch, R.H. Holm, J. Am. Chem. Soc., 88 (1966) 5201-5209.
[56] Z. Bardodej, Collect. Czech. Chem. Commun., 20 (1955) 176-179.
[57] G.S. Hall, R.H. Soderberg, Inorg. Chem., 7 (1968) 2300-2303.
[58] M.G. Miles, J.D. Wilson, Inorg. Chem., 14 (1975) 2357-2360.
[59] H.-Y. Cheng, C.-C. Lin, B.-C. Tzeng, S.-M. Peng, J. Chin. Chem. Soc., 41 (1994) 775-781.
[60] G.G. Christoph, V.L. Goedken, J. Am. Chem. Soc., 95 (1973) 3869-3875.
[61] L.F. Warren, Inorg. Chem., 16 (1977) 2814-2819.
[62] T. Ito, N. Tanaka, I. Hanazaki, S. Nagakura, Bull. Chem. Soc. Jpn., 41 (1968) 365-373.

[63] J. Rusanova, E. Rusanov, S.I. Gorelsky, D. Christendat, R. Popescu, A.A. Farah, R. Beaulac, C. Reber, A.B.P. Lever, Inorg. Chem., 45 (2006) 6246-6262.
[64] D. Kalinina, C. Dares, H. Kaluarachchi, P.G. Potvin, A.B.P. Lever, Inorg. Chem., 47 (2008) 10110-10126.
[65] M. Kapovsky, C. Dares, E.S. Dodsworth, R.A. Begum, V. Raco, A.B.P. Lever, Inorg. Chem., 52 (2013) 169-181.
[66] H.-Y. Cheng, S.-M. Peng, Inorg. Chim. Acta, 169 (1990) 23-24.
[67] B. Milliken, L. Borer, J. Russell, M. Bilich, M.M. Olmstead, Inorg. Chim. Acta, 348 (2003) 212-216.
[68] H. Masui, A.B.P. Lever, E.S. Dodsworth, Inorg. Chem., 32 (1993) 258-267.
[69] T. Jüstel, J. Bendix, N. Metzler-Nolte, T. Weyhermüller, B. Nuber, K. Wieghardt, Inorg. Chem., 37 (1998) 35-43.
[70] S.K. Dutta, U. Beckmann, E. Bill, T. Weyhermüller, K. Wieghardt, Inorg. Chem., 39 (2000) 3355-3364.
[71] D. Herebian, K.E. Wieghardt, F. Neese, J. Am. Chem. Soc., 125 (2003) 10997-11005.
[72] E. Bill, E. Bothe, P. Chaudhuri, K. Chlopek, D. Herebian, S. Kokatam, K. Ray, T. Weyhermüller, F. Neese, K. Wieghardt, Chem. Eur. J., 11 (2005) 204-224.
[73] K. Chłopek, E. Bothe, F. Neese, T. Weyhermüller, K. Wieghardt, Inorg. Chem., 45 (2006) 6298-6307.
[74] M.M. Khusniyarov, T. Weyhermüller, E. Bill, K. Wieghardt, J. Am. Chem. Soc., 131 (2009) 1208-1221.
[75] R. Nietzki, E. Hagenbach, Chem. Ber., 20 (1887) 328-338.
[76] R. Nietzki, Chem. Ber., 20 (1887) 2114-2118.
[77] K. Ujike, S. Kudoh, M. Nakata, Chem. Phys. Lett., 409 (2005) 52-56.
[78] H. Audi, Z. Chen, A. Charaf-Eddin, A. D'Aleo, G. Canard, D. Jacquemin, O. Siri, Chem. Commun., 50 (2014) 15140-15143.
[79] R. Nietzki, Chimie des matières colorantes organiques, Hachette, 1901.
[80] C. Kimich, Chem. Ber., 8 (1875) 1026-1032.
[81] O. Fischer, E. Hepp, Chem. Ber., 21 (1888) 676-684.
[82] E.v. Bandrowski, Monatsh. Chem., 10 (1889) 123-128.
[83] A.G. Green, J. Chem. Soc., Trans., 103 (1913) 925-933.
[84] W.M. Lauer, C.J. Sunde, J. Org. Chem., 03 (1938) 261-264.
[85] C.J. Sunde, W.M. Lauer, J. Org. Chem., 17 (1952) 609-612.
[86] H.E. Cox, Analyst, 58 (1933) 738-748.
[87] H.E. Cox, Analyst, 59 (1934) 3-11.
[88] M. Altman, M.M. Rieger, J. Soc. Cosmetic Chemists, 19 (1968) 141-148.
[89] K. Ohno, H. Maruyama, T. Fujihara, A. Nagasawa, Acta Crystallogr. E, 70 (2014) o303-o304.
[90] A.J. Blake, P. Hubberstey, D.J. Quinlan, Acta Crystallogr. C, 52 (1996) 1774-1776.
[91] K. Ohno, T. Fujihara, A. Nagasawa, Acta Crystallogr. E, 70 (2014) o495-o496.
[92] O. Siri, P. Braunstein, Chem. Commun., (2000) 2223-2224.
[93] O. Siri, P. Braunstein, M.-M. Rohmer, M. Bénard, R. Welter, J. Am. Chem. Soc., 125 (2003) 13793-13803.
[94] C. Seillan, P. Braunstein, O. Siri, Eur. J. Org. Chem., 2008 (2008) 3113-3117.
[95] T. Wenderski, K.M. Light, D. Ogrin, S.G. Bott, C.J. Harlan, Tetrahedron Lett., 45 (2004) 6851-6853.
[96] D.M. Khramov, A.J. Boydston, C.W. Bielawski, Org. Lett., 8 (2006) 1831-1834.
[97] K. Ohno, A. Nagasawa, T. Fujihara, Dalton Trans., 44 (2015) 368-376.
[98] M. Abdelhameed, A. Langlois, D. Fortin, P.-L. Karsenti, P.D. Harvey, Chem. Commun., 50 (2014) 11214-11217.
[99] H. Lei, S.M. Aly, P.-L. Karsenti, D. Fortin, P.D. Harvey, Organometallics, 36 (2017) 572-581.
[100] J. Andeme Edzang, Z. Chen, H. Audi, G. Canard, O. Siri, Org. Lett., 18 (2016) 5340-5343.
[101] K. Elbl, C. Krieger, H.A. Staab, Angew. Chem. Int. Ed., 25 (1986) 1023-1024.
[102] C.J. Adams, R.C. da Costa, R. Edge, D.H. Evans, M.F. Hood, J. Org. Chem., 75 (2010) 1168-1178.
[103] A. Peters, E. Kaifer, H.-J. Himmel, Eur. J. Org. Chem., 2008 (2008) 5907-5914.
[104] C. Kitamura, S. Tanaka, Y. Yamashita, Chem. Mater., 8 (1996) 570-578.
[105] F. Zhang, J. Bijleveld, E. Perzon, K. Tvingstedt, S. Barrau, O. Inganas, M.R. Andersson, J. Mater. Chem., 18 (2008) 5468-5474.

[106] A.P. Zoombelt, M. Fonrodona, M.G.R. Turbiez, M.M. Wienk, R.A.J. Janssen, J. Mater. Chem., 19 (2009) 5336-5342.
[107] E. Wang, L. Hou, Z. Wang, S. Hellström, W. Mammo, F. Zhang, O. Inganäs, M.R. Andersson, Org. Lett., 12 (2010) 4470-4473.
[108] L.-P. Zhang, K.-J. Jiang, G. Li, Q.-Q. Zhang, L.-M. Yang, J. Mater. Chem. A, 2 (2014) 14852-14857.
[109] P. Biegger, M. Schaffroth, K. Brodner, O. Tverskoy, F. Rominger, U.H.F. Bunz, Chem. Commun., 51 (2015) 14844-14847.
[110] B.D. Lindner, F. Paulus, A.L. Appleton, M. Schaffroth, J.U. Engelhart, K.M. Schelkle, O. Tverskoy, F. Rominger, M. Hamburger, U.H.F. Bunz, Journal of Materials Chemistry C, 2 (2014) 9609-9612.
[111] T.L. Tam, H. Li, F. Wei, K.J. Tan, C. Kloc, Y.M. Lam, S.G. Mhaisalkar, A.C. Grimsdale, Org. Lett., 12 (2010) 3340-3343.
[112] J. Zhang, T.C. Parker, W. Chen, L. Williams, V.N. Khrustalev, E.V. Jucov, S. Barlow, T.V. Timofeeva, S.R. Marder, J. Org. Chem., 81 (2016) 360-370.
[113] H. Rumpel, H.H. Limbach, J. Am. Chem. Soc., 111 (1989) 5429-5441.
[114] S. Dähne, D. Leupold, Angew. Chem. Int. Ed., 5 (1966) 984-993.
[115] M. Elhabiri, O. Siri, A. Sornosa-Tent, A.-M. Albrecht-Gary, P. Braunstein, Chem. Eur. J., 10 (2004) 134-141.
[116] I.-R. Jeon, J.G. Park, D.J. Xiao, T.D. Harris, J. Am. Chem. Soc., 135 (2013) 16845-16848.
[117] J.-P. Taquet, O. Siri, J.-P. Collin, A. Messaoudi, P. Braunstein, N. J. Chem., 29 (2005) 188-192.
[118] H. Masui, A.L. Freda, M.C. Zerner, A.B.P. Lever, Inorg. Chem., 39 (2000) 141-152.
[119] D. Kumbhakar, B. Sarkar, A. Das, A.K. Das, S.M. Mobin, J. Fiedler, W. Kaim, G.K. Lahiri, Dalton Trans., (2009) 9645-9652.
[120] J. Rall, A.F. Stange, K. Hübler, W. Kaim, Angew. Chem. Int. Ed., 37 (1998) 2681-2682.
[121] S. Frantz, J. Rall, I. Hartenbach, T. Schleid, S. Záliš, W. Kaim, Chem. Eur. J., 10 (2004) 149-154.
[122] P. Braunstein, A. Demessence, O. Siri, J.-P. Taquet, C. R. Chim., 7 (2004) 909-913.
[123] K. Ohno, T. Fujihara, A. Nagasawa, Polyhedron, 81 (2014) 715-722.
[124] H.-Y. Cheng, G.-H. Lee, S.-M. Peng, Inorg. Chim. Acta, 191 (1992) 25-27.
[125] S. Krupski, J.V. Dickschat, A. Hepp, T. Pape, F.E. Hahn, Organometallics, 31 (2012) 2078-2084.
[126] A. Peters, C. Trumm, M. Reinmuth, D. Emeljanenko, E. Kaifer, H.-J. Himmel, Eur. J. Inorg. Chem., 2009 (2009) 3791-3800.
[127] C. Trumm, O. Hübner, E. Kaifer, H.-J. Himmel, Eur. J. Inorg. Chem., 2010 (2010) 3102-3108.
[128] D. Emeljanenko, A. Peters, N. Wagner, J. Beck, E. Kaifer, H.-J. Himmel, Eur. J. Inorg. Chem., 2010 (2010) 1839-1846.
[129] S. Stang, A. Lebkücher, P. Walter, E. Kaifer, H.-J. Himmel, Eur. J. Inorg. Chem., 2012 (2012) 4833-4845.
[130] C. Trumm, S. Stang, B. Eberle, E. Kaifer, N. Wagner, J. Beck, T. Bredow, N. Meyerbröker, M. Zharnikov, O. Hübner, H.-J. Himmel, Eur. J. Inorg. Chem., 2012 (2012) 3156-3167.
[131] J.-P. Taquet, O. Siri, P. Braunstein, R. Welter, Inorg. Chem., 45 (2006) 4668-4676.
[132] O. Siri, J.-P. Taquet, J.-P. Collin, M.-M. Rohmer, M. Bénard, P. Braunstein, Chem. Eur. J., 11 (2005) 7247-7253.
[133] M.B. Robin, P. Day, Adv. Inorg. Chem. Radiochem., 10 (1968) 247-422.
[134] Y.-B. Huang, G.-R. Tang, G.-Y. Jin, G.-X. Jin, Organometallics, 27 (2008) 259-269.
[135] Y. Su, Y. Zhao, J. Gao, Q. Dong, B. Wu, X.-J. Yang, Inorg. Chem., 51 (2012) 5889-5896.
[136] D. Schweinfurth, M.M. Khusniyarov, D. Bubrin, S. Hohloch, C.-Y. Su, B. Sarkar, Inorg. Chem., 52 (2013) 10332-10339.
[137] N. Deibel, M.G. Sommer, S. Hohloch, J. Schwann, D. Schweinfurth, F. Ehret, B. Sarkar, Organometallics, 33 (2014) 4756-4765.
[138] J.A. DeGayner, I.-R. Jeon, T.D. Harris, Chem. Sci., 6 (2015) 6639-6648.
[139] O. Siri, P. Braunstein, J.-P. Taquet, J.-P. Collin, R. Welter, Dalton Trans., (2007) 1481-1483.